Ultrafast exciton-exciton coherent transfer in molecular aggregates and its application to light-harvesting systems

Kim Hyeon-Deuk[a] and Yoshitaka Tanimura
Department of Chemistry, Kyoto University, Kyoto 606-8502, Japan

Minheang Cho[b]
Department of Chemistry, Korea University, Seoul 136-701, Korea;
Center for Multidimensional Spectroscopy, Korea University, Seoul 136-701, Korea;
and Multidimensional Spectroscopy Laboratory, Korea Basic Science Institute, Seoul 136-701, Korea

(Received 7 March 2007; accepted 6 June 2007; published online 15 August 2007)

Effects of the exciton-exciton coherence transfer (EECT) in strongly coupled molecular aggregates are investigated from the reduced time-evolution equation which we have developed to describe EECT. Starting with the nonlinear response function, we obtained explicit contributions from EECT to four-wave-mixing spectrum such as photon echo, taking into account double exciton states, static disorder, and heat-bath coupling represented by arbitrary spectral densities. By using the doorway-window picture and the projection operator technique, the transfer rates between two different electronic coherent states are obtained within a framework of cumulant expansion at high temperature. Applications of the present theory to strongly coupled B850 chlorophylls in the photosynthetic light harvesting system II (LH2) are discussed. It is shown that EECT is indispensable in properly describing ultrafast phenomena of strongly coupled molecular aggregates such as LH2 and that the EECT contribution to the two-dimensional optical spectroscopy is not negligible. © *2007 American Institute of Physics*. [DOI: 10.1063/1.2754680]

I. INTRODUCTION

Photosynthetic antenna complexes in purple bacteria show nonequilibrium transport phenomena in ultrafast time scales.[1] Such ultrafast transfers are rationalized by utilizing quantum mechanics ingeniously.[2] Actually, while the Förster theory provides a good description of excitation transfers between monomers,[3] exciton transfer theories beyond the Förster theory had been needed and proposed.[4–8] It is also well known that the Redfield theory does not usually satisfy the indispensable positivity condition,[9–12] and that it has some limitations in describing exciton transfers.[7,12] In particular, for the population transfer process, the direct comparison of the Redfield theory with the exciton population transfer (EPT) was performed, and it was concluded that the two are different and the former has a certain limitation even in describing EPT.[7] Furthermore, as reported in Ref. 12, the weak diagonal exciton-photon coupling approximation invoked in the Redfield theory is based on the notion that the bath degrees of freedom with high frequencies are frozen and that a typical transfer time scale should be longer than several tens of femtoseconds. The latter condition may not be satisfied in the cases of light-harvesting complexes because the exciton transfer process is often very fast.

A variety of ultrafast nonlinear spectroscopic methods have been used to elucidate the underlying physics of the ultrafast transfer phenomena and their mechanisms. Previous works assumed weak exciton-phonon couplings and paid attention to comparatively slow population relaxation dynamics. Meier *et al.* considered strong diagonal exciton-phonon couplings by introducing the exciton basis, where the system-bath interaction was represented by arbitrary spectral densities.[13] Since the diagonal exciton-phonon coupling was treated nonperturbatively, the polaron formation and the nuclear reorganization energies were properly incorporated. However, due to the neglect of the off-diagonal exciton-phonon coupling inducing exciton transfers, their theory can be applied only to the case when the exciton migration is not important. Such experiment and simulation studies on peripheral light harvesting complexes I and II (LH1 and LH2) were performed by Fleming and co-workers, and they tried to analyze the experimental data theoretically by introducing spectral densities characterizing the diagonal exciton-phonon coupling.[14–16]

One of the most important nonequilibrium phenomena in molecular aggregates is EPT. Zhang *et al.* included the off-diagonal exciton-phonon coupling perturbatively and obtained the corresponding nonlinear response function allowing them to numerically calculate the signals of LH2 antenna complexes.[17] Experimental studies on EPT were performed later. The theory of Zhang *et al.* was found to be successful for interpreting experimental data. Recently, the exciton theory for a coupled multichromophore system was developed and shown to be useful in describing two-dimensional electronic spectroscopy of the Fenna-Matthews-Olson light-harvesting complex.[18,19]

Another critical nonequilibrium transfer that has not been studied in detail is the exciton-excition coherence transfer (EECT) between different electronic coherent states. EECT occurs only within ultrafast time scales because of the

[a]Electronic mail: kim@kuchem.kyoto-u.ac.jp
[b]Electronic mail: mcho@korea.ac.kr

instability of coherent states and could not be observed in previous spectroscopic experiments, so that there have been few efforts to study EECT. However, recent nonlinear optical spectroscopy utilizing femtosecond laser pulses allows us to detect such ultrafast dynamics in molecules. This motivated us to derive a coupled integrodifferential equation for EECT and to investigate an explicit contribution to the nonlinear response function. Therefore, the principle goal of this work is to develop a transport theory of both EPT and EECT processes in strongly coupled multichromophore systems, including effects of colored noise and its nonlinear response function.

This paper is organized as follows. In Sec. II, we introduce the Frenkel-exciton Hamiltonian in the site representation and recast it to the corresponding exciton representation. The nonlinear response function including EECT processes is discussed in Sec. III and expanded by using the projection operator method in Sec. III A. We use the doorway-window picture of the third-order response function in Sec. III B. The time-evolution equation of the Green's function for EECT is presented in Sec. IV. The explicit doorway-window functions and the Green's function are given in Sec. V, and the second-order cumulant expansion expressions are presented in Sec. VI. In Sec. VII, an explicit kernel function of the Green's function of EECT is discussed. The analytical results of the four-wave-mixing signal are given in Sec. VIII. The application to the LH2 antenna system is presented in Sec. IX, and numerically calculated signals are compared with the previous result reported by Zhang *et al.*[17] The main results are summarized in Sec. X.

II. EXCITON HAMILTONIANS

We consider a coupled multichromophore system consisting of N two-level monomers.[17,19,20] The Frenkel-exciton Hamiltonian is given by

$$\hat{H} = \sum_n \Omega_n \hat{M}_n^\dagger \hat{M}_n + \sum_{m,n}^{m\neq n} J_{mn} \hat{M}_m^\dagger \hat{M}_n + \sum_{m,n} q_{mn}^{(c)} \hat{M}_m^\dagger \hat{M}_n + H_{\mathrm{ph}}(\{q_j\}), \tag{1}$$

where $\hat{M}_n^\dagger$ and $\hat{M}_n$ are the creation and annihilation operators for the nth monomer excitation; J_{mn} denotes the coupling constant between monomers m and n. We assume that the system is coupled to the harmonic heat bath

$$H_{\mathrm{ph}}(\{q_j\}) = \sum_j \left(\frac{p_j^2}{2m_j} + \frac{m_j \omega_j^2 q_j^2}{2} \right). \tag{2}$$

The coupling coefficient $q_{mn}^{(c)}$ is composed of the collective bath coordinates, responsible for the monomer-phonon coupling,

$$q_{mn}^{(c)} = \sum_j m_j \omega_j^2 z_{j,mn} q_j. \tag{3}$$

$z_{j,mn}$ is the coupling strength of the jth phonon to the excitation variable $\hat{M}_m^\dagger \hat{M}_n$. Note that $z_{j,mn}$ is proportional to the product of wave functions of mth and nth excited chromophores, $\phi_m \phi_n^*$.

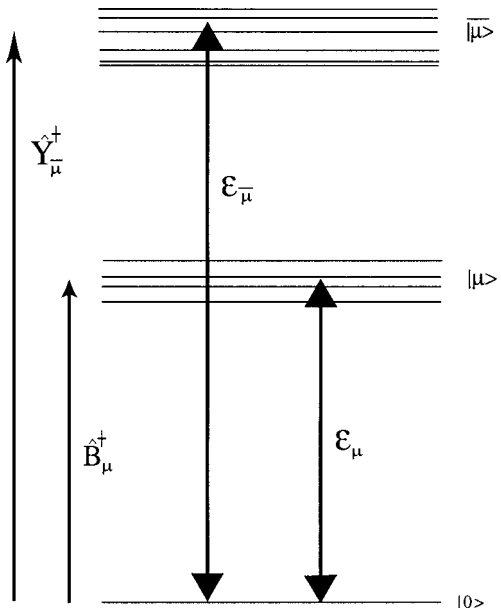

FIG. 1. Exciton level-structure of the Hamiltonian [Eq. (5)]. $|0\rangle$ is the ground state, while $|\mu\rangle$ means one of the one-exciton levels consisting of N states. $|\bar{\mu}\rangle$ denotes one of the $N(N-1)/2$ two-exciton states. ϵ_μ and $\epsilon_{\bar{\mu}}$ are eigenenergies for the single and double excitons, respectively. The exciton eigenenergies ϵ_μ are numerically obtained by diagonalizing the first and second terms of the Frenkel-exciton Hamiltonian [Eq. (1)] (Ref. 19). Its monomer excitation energies Ω_m are specified by the Gaussian distribution [Eq. (77)]. For example, the characteristic eigenenergy of B850 chlorophylls $\tilde{\Omega}_m = 11\,710\ \mathrm{cm}^{-1}$ and the full width at half maximum $\sigma = 2\sqrt{\log 2}\tilde{\Omega}_m = 325\ \mathrm{cm}^{-1}$.

We recast the Hamiltonian [Eq. (1)] consisting of N well-separated manifolds to the corresponding exciton representation.[19] The third-order response function for four-wave-mixing spectroscopy involves transitions among the ground state ($|0\rangle$), the single exciton states ($|\mu\rangle$), and the double exciton states ($|\bar{\mu}\rangle$), as shown in Fig. 1. Thus, the Hamiltonian [Eq. (1)] can be rearranged as

$$\hat{H}_e = \hat{H}_0 + \hat{H}_1, \tag{4}$$

where the nonperturbative term is

$$\hat{H}_0 = \sum_\mu \epsilon_\mu \hat{B}_\mu^\dagger \hat{B}_\mu + \sum_{\bar{\mu}} \epsilon_{\bar{\mu}} \hat{Y}_{\bar{\mu}}^\dagger \hat{Y}_{\bar{\mu}} + \sum_\mu q_{\mu\mu}^{(c)} \hat{B}_\mu^\dagger \hat{B}_\mu + \sum_{\bar{\mu}} q_{\bar{\mu}\bar{\mu}}^{(c)} \hat{Y}_{\bar{\mu}}^\dagger \hat{Y}_{\bar{\mu}} + H_{\mathrm{ph}}(\{q_j\}) \tag{5}$$

and the perturbative term is

$$\hat{H}_1 = \sum_{\mu,\nu}^{\mu\neq\nu} q_{\mu\nu}^{(c)} \hat{B}_\mu^\dagger \hat{B}_\nu + \sum_{\bar{\mu},\bar{\nu}}^{\bar{\mu}\neq\bar{\nu}} q_{\bar{\mu}\bar{\nu}}^{(c)} \hat{Y}_{\bar{\mu}}^\dagger \hat{Y}_{\bar{\nu}}. \tag{6}$$

$\hat{B}_\mu^\dagger$ and $\hat{B}_\mu$ are the exciton creation and annihilation operators for the single exciton μ, while the corresponding operators for the double exciton $\bar{\mu}$ are $\hat{Y}_{\bar{\mu}}^\dagger$ and $\hat{Y}_{\bar{\mu}}$, respectively. ϵ_μ and $\epsilon_{\bar{\mu}}$ denote eigenenergies for the excitons μ and $\bar{\mu}$, respectively. The exciton-phonon coupling makes the exciton eigenenergies fluctuate by $q_{\mu\mu}^{(c)}$ and $q_{\bar{\mu}\bar{\mu}}^{(c)}$, and it also generates exciton transfers by $q_{\mu\nu}^{(c)}$ and $q_{\bar{\mu}\bar{\nu}}^{(c)}$. Their explicit forms are given in Ref. 19.

III. NONLINEAR RESPONSE FUNCTION

Let us introduce the third-order response function, which is indispensable in calculating four-wave-mixing signals since it is directly related to spectroscopic observables. The third-order response function can be written as[21]

$$R^{(3)}(t_3,t_2,t_1) = i^3 \,\mathrm{Tr}[\hat{d}\hat{G}(t_3)\hat{d}^{\times}\hat{G}(t_2)\hat{d}^{\times}\hat{G}(t_1)\hat{d}^{\times}\hat{\rho}_{00}], \quad (7)$$

where the equilibrium density matrix in the ground state is assumed to be

$$\hat{\rho}_{00} = |0\rangle \frac{\exp[-\beta H_{\mathrm{ph}}(\{q_j\})]}{Z}\langle 0|, \quad (8)$$

with $\beta = 1/k_B T_B$ and the normalization constant Z; k_B and T_B are the Boltzmann constant and the temperature, respectively. The Liouville path propagator is defined by

$$\hat{G}(t) \equiv \exp[-i\hat{L}t], \quad (9)$$

with $\hat{L}\hat{X} = [\hat{H}_e, \hat{X}]$, and $\hat{d}^{\times}$ is the hyperoperator of dipole defined by

$$\hat{d}^{\times}\hat{X} \equiv \hat{d}\hat{X} - \hat{X}\hat{d} \quad (10)$$

for any operator $\hat{X}$. The dipole operator within the exciton representation has the form

$$\hat{d} = \sum_{\mu} d_{\mu}(\hat{B}_{\mu} + \hat{B}_{\mu}^{\dagger}) + \sum_{\mu,\bar{\mu}} d_{\mu,\bar{\mu}}(\hat{Y}_{\bar{\mu}}^{\dagger}\hat{B}_{\mu} + \hat{B}_{\mu}^{\dagger}\hat{Y}_{\bar{\mu}}), \quad (11)$$

where

$$d_{\mu} = \sum_{m} d_m \phi_{\mu}(m) \quad (12)$$

and

$$d_{\mu,\bar{\mu}} = \sum_{m=1}^{N-1}\sum_{n=m+1}^{N} \Psi_{\bar{\mu}}(m,n)\{\phi_{\mu}(n)d_m + \phi_{\mu}(m)d_n\}. \quad (13)$$

Here, $\phi_{\mu}(m)$ and $\Psi_{\bar{\mu}}(m,n)$ represent the one-exciton and two-exciton wave functions.

A. Projection operator expression

In order to calculate the third-order response function, we have to formulate time evolutions of the diagonal and off-diagonal density operators such as $\hat{\rho}_{00}(\{q_j\})$, $\hat{\rho}_{0\mu}(\{q_j\})$, $\hat{\rho}_{0\bar{\mu}}(\{q_j\})$, $\hat{\rho}_{\mu\nu}(\{q_j\})$, and $\hat{\rho}_{\mu\bar{\mu}}(\{q_j\})$. It is useful to introduce the projection operators as follows. The operator that extracts the diagonal component of $\hat{\rho}(\{q_j\})$ is defined by

$$\mathsf{P}_{\mu}\hat{\rho} \equiv \hat{\rho}_{\mu\mu}\,\mathrm{Tr}_{\{q_j\}}\{\hat{\rho}_{\mu\mu}\}, \quad (14)$$

where the equilibrium density matrix in the μth exciton is

$$\hat{\rho}_{\mu\mu} = |\mu\rangle \frac{\exp[-\beta H_{\mu}(\{q_j\})]}{Z}\langle\mu|. \quad (15)$$

Similarly, the operator giving rise to the ground state population component is

$$\mathsf{P}_0\hat{\rho} \equiv \hat{\rho}_{00}\,\mathrm{Tr}_{\{q_j\}}[\hat{\rho}_{00}]. \quad (16)$$

The total operator is therefore given by

$$\mathsf{P} = \mathsf{P}_0 + \sum_{\mu}\mathsf{P}_{\mu}. \quad (17)$$

We next define the complementary operator, which projects a density matrix onto the manifold of off-diagonal components,

$$\mathsf{Q} \equiv 1 - \mathsf{P}. \quad (18)$$

EPT processes are related to the P operator dynamics as shown in Ref. 17, while, in this study, we shall focus on the nonequilibrium dynamics extracted by Q.

Since $\mathsf{P}+\mathsf{Q}=1$, we have

$$\hat{G}(t_2) = (\mathsf{P}+\mathsf{Q})\hat{G}(t_2)(\mathsf{P}+\mathsf{Q}) \quad (19)$$

$$= \hat{G}_{\mathsf{PP}}(t_2) + \hat{G}_{\mathsf{PQ}}(t_2) + \hat{G}_{\mathsf{QP}}(t_2) + \hat{G}_{\mathsf{QQ}}(t_2), \quad (20)$$

where $\hat{G}_{\mathsf{AB}}(t) \equiv \mathsf{A}\hat{G}(t)\mathsf{B}$. Explicit expressions of the above terms are presented in Appendix A. In order to obtain them, we divide the full Liouville operator $\hat{L}$ into the perturbative and nonperturbative contributions:

$$\hat{L} = \hat{L}_0 + \hat{L}_1. \quad (21)$$

Substitution of $\hat{G}(t_2)$ into Eq. (7) leads to

$$\begin{aligned} R^{(3)}(t_3,t_2,t_1) &= i^3\,\mathrm{Tr}[\hat{d}\hat{G}_{\mathsf{QQ}}(t_3)\hat{d}^{\times}\hat{G}_{\mathsf{PP}}(t_2)\hat{d}^{\times}\hat{G}_{\mathsf{QQ}}(t_1)\hat{d}^{\times}\hat{\rho}_{00}] \\ &+ i^3\,\mathrm{Tr}[\hat{d}\hat{G}_{\mathsf{QQ}}(t_3)\hat{d}^{\times}\hat{G}_{\mathsf{PQ}}(t_2)\hat{d}^{\times}\hat{G}_{\mathsf{QQ}}(t_1)\hat{d}^{\times}\hat{\rho}_{00}] \\ &+ i^3\,\mathrm{Tr}[\hat{d}\hat{G}_{\mathsf{QQ}}(t_3)\hat{d}^{\times}\hat{G}_{\mathsf{QP}}(t_2)\hat{d}^{\times}\hat{G}_{\mathsf{QQ}}(t_1)\hat{d}^{\times}\hat{\rho}_{00}] \\ &+ i^3\,\mathrm{Tr}[\hat{d}\hat{G}_{\mathsf{QQ}}(t_3)\hat{d}^{\times}\hat{G}_{\mathsf{QQ}}(t_2)\hat{d}^{\times}\hat{G}_{\mathsf{QQ}}(t_1)\hat{d}^{\times}\hat{\rho}_{00}]. \end{aligned} \quad (22)$$

We note that during t_1 and t_3, the density matrix is always in a coherent state such as $\rho_{0\mu}$, $\rho_{0\bar{\mu}}$, $\rho_{\mu\nu}$, and $\rho_{\mu\bar{\nu}}$. Therefore, only $\hat{G}_{\mathsf{QQ}}(t)$ appears during t_1 and t_3. To the lowest order of $\hat{L}_1$, using the results in Appendix A, we have

$$\begin{aligned} R^{(3)}(t_3,t_2,t_1) &= i^3\,\mathrm{Tr}[\hat{d}\hat{G}_{\mathsf{QQ}}(t_3)\hat{d}^{\times}\hat{G}^0_{\mathsf{PP}}(t_2)\hat{d}^{\times}\hat{G}_{\mathsf{QQ}}(t_1)\hat{d}^{\times}\hat{\rho}_{00}] \\ &+ i^3\,\mathrm{Tr}[\hat{d}\hat{G}_{\mathsf{QQ}}(t_3)\hat{d}^{\times}\hat{G}_{\mathsf{QQ}}(t_2)\hat{d}^{\times}\hat{G}_{\mathsf{QQ}}(t_1)\hat{d}^{\times}\hat{\rho}_{00}], \end{aligned} \quad (23)$$

in terms of $\hat{G}_{QQ}(t_2)$ with $\hat{G}^0_{\mathsf{AB}}(t) = \mathsf{A}\exp[-i\hat{L}_0 t]\mathsf{B}$. The first term in Eq. (23) becomes

$$i^3\,\mathrm{Tr}[\hat{d}\hat{G}_{\mathsf{QQ}}(t_3)\hat{d}^{\times}\hat{G}^0_{\mathsf{PP}}(t_2)\hat{d}^{\times}\hat{G}_{\mathsf{QQ}}(t_1)\hat{d}^{\times}\hat{\rho}_{00}] \quad (24)$$

$$= R^{(3)}(t_3,\infty,t_1), \quad (25)$$

where $R^{(3)}(t_3,\infty,t_1)$ is identical with the second and third terms in Eq. (B9) of Ref. 17 and corresponds to Eq. (D7) with $t_2=0$ in Ref. 17. Thus, we will not consider the first term of Eq. (23) in detail in the present study.

B. The doorway-window expression

The second term in Eq. (23), which includes the EECT, can be rewritten as

$$R^{(3)}(t_3,t_2,t_1) = i^3 \sum_{\lambda,\lambda'} \mathrm{Tr}[\hat{d}\hat{G}_{\mathrm{QQ}}(t_3)\hat{d}^{\times}\mathsf{Q}_{\lambda}\hat{G}(t_2)\mathsf{Q}_{\lambda'}\hat{d}^{\times}\hat{G}_{\mathrm{QQ}}(t_1)\hat{d}^{\times}\hat{\rho}_{00}] \tag{26}$$

$$= -i\sum_{\lambda,\lambda'} \mathrm{Tr}[\hat{d}\hat{G}_{\mathrm{QQ}}(t_3)\hat{d}^{\times}\hat{G}_{\lambda\lambda'}(t_2)\hat{d}^{\times}\hat{G}_{\mathrm{QQ}}(t_1)\hat{d}^{\times}\hat{\rho}_{00}] \tag{27}$$

$$\simeq -\sum_{\lambda,\lambda'} W_{\lambda}(t_3)\tilde{G}_{\lambda\lambda'}(t_2)D_{\lambda'}(t_1). \tag{28}$$

It should be mentioned that all the single exciton coherence transfers (SECTs) during t_1 and t_3 can be ignored, as shown in Appendix B. λ and λ' denote coherent states such as $\rho_{0\mu}$, $\rho_{0\bar{\mu}}$, $\rho_{\mu\nu}$, and $\rho_{\mu\bar{\mu}}$. In Eq. (28), we introduced the doorway function

$$D_{\lambda'}(t_1) \equiv \mathrm{Tr}[\lambda'^{\dagger}\hat{d}^{\times}\hat{G}_{\mathrm{QQ}}(t_1)\hat{d}^{\times}\hat{\rho}_{00}] \tag{29}$$

and the window function

$$W_{\lambda}(t_3) \equiv \mathrm{Tr}[\hat{d}\hat{G}_{\mathrm{QQ}}(t_3)\hat{d}^{\times}\hat{\rho}_{\lambda}]. \tag{30}$$

$\lambda'^{\dagger}$ in the doorway function is needed to generate $\hat{\rho}_{\lambda'}$ in the Green's function. The Green's function describing EECT, defined as

$$\hat{G}_{\lambda\lambda'}(t_2) \equiv \mathsf{Q}_{\lambda}\hat{G}(t_2)\mathsf{Q}_{\lambda'}\hat{\rho}_{\lambda'}, \tag{31}$$

can be viewed as the conditional probability for the coherent state to be in λ at time t_2 when it starts at λ' at time $t_2=0$. We further introduce

$$\tilde{\hat{G}}_{\lambda\lambda'}(t_2) \equiv \lambda^{\dagger}\hat{G}_{\lambda\lambda'}(t_2) \tag{32}$$

since $\lambda^{\dagger}$ is necessary to produce $\hat{\rho}_{\lambda}$ in the window function.

IV. THE TIME-EVOLUTION EQUATION OF THE GREEN'S FUNCTION

We start from the Liouville equation of the whole system,

$$\frac{\partial\rho(t)}{\partial t} = -i\hat{L}\rho(t). \tag{33}$$

Using the projection operator method,[22,23] we obtain

$$\frac{\partial\mathsf{Q}\rho(t)}{\partial t} = -i\mathsf{Q}\hat{L}\mathsf{Q}\rho(t) - \mathsf{Q}\hat{L}\int_0^t d\tau e^{-i(t-\tau)\mathsf{P}\hat{L}}\mathsf{P}\hat{L}\mathsf{Q}\rho(\tau) - i\mathsf{Q}\hat{L}e^{-it\mathsf{P}\hat{L}}\mathsf{P}\rho(0). \tag{34}$$

This equation can also be derived by interchanging P and Q in Eq. (9) of Ref. 7. At time $t_2=0$, the density matrix must be in a coherent state for EECT, so that we can set $\mathsf{P}\rho(0)=0$. Equation (34) leads to

$$\frac{\partial\mathsf{Q}\rho(t)}{\partial t} = -i\mathsf{Q}\hat{L}\mathsf{Q}\rho(t) - \mathsf{Q}\hat{L}\int_0^t d\tau e^{-i(t-\tau)\mathsf{P}\hat{L}_1}\mathsf{P}\hat{L}_1\mathsf{Q}\rho(\tau) \tag{35}$$

$$= -i\mathsf{Q}\hat{L}\mathsf{Q}\rho(t) - \int_0^t d\tau\mathsf{Q}\hat{L}_1\mathsf{P}\hat{L}_1\mathsf{Q}\rho(\tau). \tag{36}$$

Here, we used the formula $\hat{L}_0\mathsf{P}=\mathsf{P}\hat{L}_0=0$ and $\mathsf{P}\hat{L}_1\mathsf{P}=0$. To zeroth order of $\hat{L}_1$, the above equation leads to

$$\frac{\partial\mathsf{Q}\rho(t)}{\partial t} = -i\mathsf{Q}\hat{L}_0\mathsf{Q}\rho(t). \tag{37}$$

This gives the zeroth-order solution $R^{(c)}(t_3,t_2,t_1)$, which is identical to Eq. (B2) of Ref. 17.

On the order hand, in order to discuss EECT, we have to treat the whole of Eq. (36). The first term in Eq. (36) involves a term that is first order of $\hat{L}_1$, which is linearly proportional to q_j. Consequently, the corresponding contribution vanishes when the kernel function is calculated by statistically averaging with respect to the harmonic bath H_{ph}. Furthermore, the remaining part of the first term, $-i\mathsf{Q}\hat{L}_0\mathsf{Q}\rho(t)$, also vanishes (see Appendix B 4). As a result, we can remove the first term in Eq. (36),

$$\frac{\partial\mathsf{Q}\rho(t)}{\partial t} = -\int_0^t d\tau\mathsf{Q}\hat{L}_1\mathsf{P}\hat{L}_1\mathsf{Q}\rho(\tau). \tag{38}$$

Replacing the left Q with Q_{λ} and $\rho(t)$ with $e^{-i\hat{L}t}\mathsf{Q}_{\lambda'}\rho(0)$, Eq. (38) can be rewritten as

$$\frac{\partial\mathsf{Q}_{\lambda}e^{-i\hat{L}t}\mathsf{Q}_{\lambda'}\rho(0)}{\partial t} = -\sum_{\alpha}\int_0^t d\tau\mathsf{Q}_{\lambda}\hat{L}_1\mathsf{P}\hat{L}_1\mathsf{Q}_{\alpha}e^{-i\hat{L}\tau}\mathsf{Q}_{\lambda'}\rho(0). \tag{39}$$

At last, the time-evolution equation of the Green's function is obtained as

$$\frac{\partial\hat{G}_{\lambda\lambda'}(t)}{\partial t} = -\sum_{\alpha}\int_0^t d\tau\mathsf{Q}_{\lambda}\hat{L}_1\mathsf{P}\hat{L}_1\hat{G}_{\alpha\lambda'}(\tau). \tag{40}$$

From the definition of $\tilde{\hat{G}}_{\lambda\lambda'}(t)$ in Eq. (32), we have

$$\frac{\partial\tilde{G}_{\lambda\lambda'}(t)}{\partial t} = \sum_{\alpha}\int_0^t d\tau K_{\lambda\alpha}\tilde{G}_{\alpha\lambda'}(\tau), \tag{41}$$

where the kernel function is found to be

$$K_{\lambda\alpha} \equiv -\mathrm{Tr}[\lambda^{\dagger}\mathsf{Q}_{\lambda}\hat{L}_1\mathsf{P}\hat{L}_1\hat{\rho}_{\alpha}]. \tag{42}$$

Due to the conservation of the total exciton number, we finally have the following time-evolution equation of $\tilde{G}_{\lambda\lambda'}(t)$:

$$\frac{\partial\tilde{G}_{\lambda\lambda'}(t)}{\partial t} = \sum_{\alpha}\int_0^t d\tau\{K_{\lambda\alpha}\tilde{G}_{\alpha\lambda'}(\tau) - K_{\alpha\gamma}\tilde{G}_{\lambda\lambda'}(\tau)\}. \tag{43}$$

One of the interesting observations in this section is that the EECT kernel does not depend on time. This has originated from Eq. (34), which is an equation of motion of the

Q-projected density operator obtained rigorously by using the projection operator technique. Unlike the case of the P-projected density operator, Eq. (38) does not have a Liouville space time-evolution operator in between $\hat{L}_1$ and $\mathsf{P}\hat{L}_1$ operators. To make this more specific let us write the corresponding equation of motion for the P-projected density operator for the sake of direct comparison,

$$\frac{\partial \mathsf{P}\rho(t)}{\partial t} = -\int_0^t d\tau \mathsf{P}\hat{L}_1 e^{-i(t-\tau)\hat{L}_0}\hat{L}_1 \mathsf{P}\rho(\tau). \tag{44}$$

The corresponding equation of motion for $\mathsf{Q}_\rho(t)$ was given in Eq. (38) by considering up to the second-order term with respect to $\hat{L}_1$, where the Liouville space time-evolution operator does not appear in this expression. This is different from that of Redfield theory.[7,24] However, one can understand this difference by examining the underlying physical processes hidden in Eqs. (38) and (44). On the right-hand side of Eq. (44), $\hat{L}_1\mathsf{P}_\rho(\tau)$ represents a coherent state (off-diagonal density matrix), $|b(\tau)\rangle\langle a(\tau)|$. Then, the time-evolution operator acts onto this coherent state such as $e^{-i(t-\tau)\hat{H}_0}|b(\tau)\rangle\langle a(\tau)|e^{i(t-\tau)\hat{H}_0}$. Since $b \neq a$, this is highly fluctuating due to the bath degrees of freedom, and its correlation time determines the time scale of the time-dependent rate kernel for the population transfer process. On the other hand, when we obtained Eq. (38), we used the formula $\hat{L}_0\mathsf{P}=\mathsf{P}\hat{L}_0=0$, which means that the diagonal density operator is commutative with the zero-order Hamiltonian, as it should be by the definition of the P operator. Noting that $\mathsf{P}\hat{L}_1\mathsf{Q}_\rho(\tau)$ on the right-hand side of Eq. (38) is a population state, any time-evolution operator acting on this, i.e., $e^{-i(t-\tau)\hat{L}_0}\mathsf{P}\hat{L}_1\mathsf{Q}_\rho(\tau)$, vanishes except for the zero-order expansion term of $e^{-i(t-\tau)\hat{L}_0}$, which is just one. Therefore, the kernel for the Q-projected density operator does not depend on time. As mentioned above, one can obtain the quantum master equation from Eq. (44) for the population states. For the Q-projected density matrix, we obtained Eq. (43) from Eq. (38). However, it is believed that Eq. (43) should not be interpreted as a conventional Markov master equation but just as a coupled integrodifferential equation. Therefore, $K_{\lambda\alpha}$ in Eq. (42) is not a Markov rate constant in a conventional sense. Note that the population state can be interpreted classically because it describes the probability of finding the system to be in a given state. However, the coherent state has no classical analog. That is to say, it is not possible to attempt to directly connect the equation of motion for the Green's function in Eq. (43), which describes the coherent state evolution in time, to a classical kinetic equation.

V. EXPLICIT EXPRESSIONS OF THE DOORWAY AND WINDOW FUNCTIONS

In Sec. III B, to obtain Eq. (28), we used the factorization approximation to rewrite the total nonlinear response function as a product of three ensemble-averaged functions that depend on the three independent time variables. In the present section, we will provide general expressions of the doorway (preparation) and window (probing) functions in terms of correlation functions of the exciton operators. The doorway function in Eq. (29) can be written as an expanded form,

$$\begin{aligned} D_{\lambda'}(t_1) = {} & \mathrm{Tr}[\lambda'^{\dagger} P \hat{G}_{\mathrm{QQ}}(t_1) P \hat{\rho}_{00}] \\ & - \mathrm{Tr}[\lambda'^{\dagger}(\hat{G}_{\mathrm{QQ}}(t_1) P \hat{\rho}_{00}) P] \\ & - \mathrm{Tr}[\lambda'^{\dagger} P(\hat{G}_{\mathrm{QQ}}(t_1)\hat{\rho}_{00} P)] \\ & + \mathrm{Tr}[\lambda'^{\dagger}(\hat{G}_{\mathrm{QQ}}(t_1)\hat{\rho}_{00} P) P]. \end{aligned} \tag{45}$$

From the fact that λ' denotes a coherent state, Eq. (45) leads to

$$\begin{aligned} D_{\lambda'}(t_1) = {} & -\delta_{a'\mu'}\delta_{b'\nu'} d_{a'} d_{b'}\, \mathrm{Tr}[(\hat{B}^{\dagger}_{a'}\hat{B}_{b'})^{\dagger}\hat{G}_{\mathrm{QQ}}(t_1)\hat{B}^{\dagger}_{a'}\hat{\rho}_{00}\hat{B}_{b'}] - \delta_{a'\mu'}\delta_{b'\nu'} d_{a'} d_{b'}\, \mathrm{Tr}[(\hat{B}^{\dagger}_{a'}\hat{B}_{b'})^{\dagger}\hat{B}^{\dagger}_{a'}\hat{G}_{\mathrm{QQ}}(t_1)\hat{\rho}_{00}\hat{B}_{b'}] \\ & + \delta_{a'\bar{\mu}'}\delta_{b'0}\sum_{c'} d_{c'} d_{c'a'}\, \mathrm{Tr}[(\hat{Y}^{\dagger}_{a'}\hat{B}_{b'})^{\dagger}\hat{Y}^{\dagger}_{a'}\hat{B}_{c'}\hat{G}_{\mathrm{QQ}}(t_1)\hat{B}^{\dagger}_{c'}\hat{\rho}_{00}] \\ & + \delta_{a'0}\delta_{b'\bar{\mu}'}\sum_{c'} d_{c'} d_{c'b'}\, \mathrm{Tr}[(\hat{B}^{\dagger}_{a'}\hat{Y}_{b'})^{\dagger}\hat{G}_{\mathrm{QQ}}(t_1)\hat{\rho}_{00}\hat{B}_{c'}\hat{B}^{\dagger}_{c'}\hat{Y}_{b'}], \end{aligned} \tag{46}$$

where we set $\lambda'=a'b'$, and the summation over λ' in Eq. (28) now corresponds to the summations over a', b', μ', ν', and $\bar{\mu}'$. Similarly, we obtain the window function

$$\begin{aligned} W_{\lambda}(t_3) = {} & \delta_{\mu a}\delta_{\nu b} d_a d_b\, \mathrm{Tr}[\hat{B}^{\dagger}_b\hat{G}_{\mathrm{QQ}}(t_3)\hat{B}_a\hat{\rho}_{ab}] + \delta_{\mu a}\delta_{\nu b}\sum_{\bar{a}} d_{a\bar{a}} d_{b\bar{a}}\, \mathrm{Tr}[\hat{B}^{\dagger}_b\hat{Y}_{\bar{a}}\hat{G}_{\mathrm{QQ}}(t_3)\hat{Y}^{\dagger}_{\bar{a}}\hat{B}_a\hat{\rho}_{ab}] - \delta_{\mu a}\delta_{\nu b} d_a d_b\, \mathrm{Tr}[\hat{B}_a\hat{G}_{\mathrm{QQ}}(t_3)\hat{\rho}_{ab}\hat{B}^{\dagger}_b] \\ & - \delta_{\mu a}\delta_{\nu b}\sum_{\bar{a}} d_{a\bar{a}} d_{b\bar{a}}\, \mathrm{Tr}[\hat{Y}^{\dagger}_{\bar{a}}\hat{B}_a\hat{G}_{\mathrm{QQ}}(t_3)\hat{\rho}_{ab}\hat{B}^{\dagger}_b\hat{Y}_{\bar{a}}] + \delta_{\bar{\mu}a}\delta_{0b}\sum_{c} d_c d_{ca}\, \mathrm{Tr}[\hat{B}_c\hat{G}_{\mathrm{QQ}}(t_3)\hat{B}^{\dagger}_c\hat{Y}_a\hat{\rho}_{ab}] \\ & + \delta_{0a}\delta_{\bar{\nu}b}\sum_{c} d_c d_{cb}\, \mathrm{Tr}[\hat{Y}^{\dagger}_b\hat{B}_c\hat{G}_{\mathrm{QQ}}(t_3)\hat{B}^{\dagger}_c\hat{\rho}_{ab}] - \delta_{\bar{\mu}a}\delta_{0b}\sum_{c} d_c d_{ca}\, \mathrm{Tr}[\hat{B}^{\dagger}_c\hat{Y}_a\hat{G}_{\mathrm{QQ}}(t_3)\hat{\rho}_{ab}\hat{B}_c] \\ & - \delta_{0a}\delta_{\bar{\nu}b}\sum_{c} d_c d_{cb}\, \mathrm{Tr}[\hat{B}^{\dagger}_c\hat{G}_{\mathrm{QQ}}(t_3)\hat{\rho}_{ab}\hat{Y}^{\dagger}_b\hat{B}_c], \end{aligned} \tag{47}$$

with $\lambda=ab$. The summation over λ in Eq. (28) corresponds to the summations over a, b, μ, ν, and $\bar{\mu}$. The above doorway and window functions can be rewritten as

$$D_{\lambda'}(t_1) = D^L_{\mu'\nu'}(t_1) + D^L_{\mu'\nu'}(-t_1) + D^L_{\bar{\mu}'}(t_1) + D^{L\dagger}_{\bar{\mu}'}(-t_1) \tag{48}$$

and

$$W_\lambda(t_3) = W^L_{\mu\nu}(t_3) - W^L_{\mu\nu}(-t_3) + W^L_{\bar{\mu}\bar{\nu}}(t_3) - W^L_{\bar{\mu}\bar{\nu}}(-t_3), \tag{49}$$

respectively. Here, the auxiliary functions in Eqs. (48) and (49) are defined as

$$D^L_{\mu'\nu'}(t_1) \equiv -\delta_{a'\mu'}\delta_{b'\nu'}d_{a'}d_{b'}\,\mathrm{Tr}[\hat{B}_{b'}\hat{B}^\dagger_{b'}\hat{B}_{a'}\hat{B}^\dagger_{a'}(t_1)\hat{\rho}_{00}], \tag{50}$$

$$D^L_{\bar{\mu}'}(t_1) \equiv \delta_{a'0}\delta_{b'\bar{\mu}'}\sum_{c'} d_{c'}d_{c'b'}\mathrm{Tr}[\hat{B}^\dagger_{a'}(-t_1)\hat{Y}_{b'}(-t_1)\hat{Y}^\dagger_{b'}(-t_1) \times \hat{B}_{c'}(-t_1)\hat{B}^\dagger_{c'}\hat{\rho}_{00}], \tag{51}$$

$$W^L_{\mu\nu}(t_3) \equiv \delta_{\mu a}\delta_{\nu b}d_a d_b\,\mathrm{Tr}[\hat{B}^\dagger_b\hat{B}_a(t_3)\hat{\rho}_{ab}] + \delta_{\mu a}\delta_{\nu b}\sum_{\bar{a}} d_{a\bar{a}}d_{b\bar{a}}\,\mathrm{Tr}[\hat{B}^\dagger_b\hat{Y}_{\bar{a}}\hat{Y}^\dagger_{\bar{a}}(t_3)\hat{B}_a(t_3)\hat{\rho}_{ab}] \tag{52}$$

$$= \delta_{\mu a}\delta_{\nu b}d_a d_b\,\mathrm{Tr}[\hat{B}_b\hat{B}^\dagger_b\hat{B}_a(t_3)\hat{B}^\dagger_a\hat{\rho}_{00}] + \delta_{\mu a}\delta_{\nu b}\sum_{\bar{a}} d_{a\bar{a}}d_{b\bar{a}}\,\mathrm{Tr}[\hat{B}_b\hat{B}^\dagger_b\hat{Y}_{\bar{a}}\hat{Y}^\dagger_{\bar{a}}(t_3)\hat{B}_a(t_3)\hat{B}^\dagger_a\hat{\rho}_{00}], \tag{53}$$

$$W^L_{\bar{\mu}\bar{\nu}}(t_3) \equiv \delta_{\bar{\mu}a}\delta_{0b}\sum_c d_c d_{ca}\,\mathrm{Tr}[\hat{B}_c\hat{B}^\dagger_c(t_3)\hat{Y}_a(t_3)\hat{\rho}_{ab}] + \delta_{0a}\delta_{\bar{\nu}b}\sum_c d_c d_{cb}\,\mathrm{Tr}[\hat{Y}^\dagger_b\hat{B}_c\hat{B}^\dagger_c(t_3)\hat{\rho}_{ab}] \tag{54}$$

$$= \delta_{\bar{\mu}a}\delta_{0b}\sum_{c,c'} d_c d_{ca}\,\mathrm{Tr}[\hat{B}_c\hat{B}^\dagger_c(t_3)\hat{Y}_a(t_3)\hat{Y}^\dagger_a\hat{B}_{c'}\hat{B}^\dagger_{c'}\hat{\rho}_{00}] + \delta_{0a}\delta_{\bar{\nu}b}\sum_{c,c'} d_c d_{cb}\,\mathrm{Tr}[\hat{B}_{c'}\hat{B}^\dagger_{c'}\hat{Y}_b\hat{Y}^\dagger_b\hat{B}_c\hat{B}^\dagger_c(t_3)\hat{\rho}_{00}], \tag{55}$$

where we used the following relations: $\hat{\rho}_{\mu\nu}=\hat{B}^\dagger_\mu\hat{\rho}_{00}\hat{B}_\nu$, $\hat{\rho}_{\bar{\mu}0}=\Sigma_\nu\hat{Y}^\dagger_{\bar{\mu}}\hat{B}_\nu\hat{B}^\dagger_\nu\hat{\rho}_{00}$, and $\hat{\rho}_{0\bar{\mu}}=\Sigma_\nu\hat{\rho}_{00}\hat{B}_\nu\hat{B}^\dagger_\nu\hat{Y}_{\bar{\mu}}$.

VI. THE SECOND-ORDER CUMULANT EXPANSION

In this section, using the second-order cumulant approximation method, we present analytical expressions for the doorway and window functions. The exciton annihilation operator in the Heisenberg representation can be expanded as

$$\hat{B}_\mu(\tau) = e^{-i\epsilon_\mu\tau}\exp_+\left[-i\int_0^\tau d\tau' q^{(c)}_{\mu\mu}(\tau')\right] \tag{56}$$

$$\simeq e^{-i\epsilon_\mu\tau}\left[1 - i\int_0^\tau d\tau' q^{(c)}_{\mu\mu}(\tau') - \int_0^\tau d\tau'\int_0^{\tau'} d\tau'' q^{(c)}_{\mu\mu}(\tau')q^{(c)}_{\mu\mu}(\tau'')\right]. \tag{57}$$

The conjugate operator can be expanded accordingly. Inserting the above expanded expressions into Eq. (50), we have

$$D^L_{\mu'\nu'}(t_1) = -\delta_{a'\mu'}\delta_{b'\nu'}d_{a'}d_{b'}e^{i\epsilon_{a'}t_1}\exp[-g_{a'a'}(-t_1)], \tag{58}$$

where the exciton line shape function $g_{\mu\nu}(t)$ is

$$g_{\mu\nu}(t) \equiv \int_0^t d\tau'\int_0^{\tau'} d\tau''\langle q^{(c)}_{\mu\mu}(\tau'')q^{(c)}_{\nu\nu}(0)\rangle \tag{59}$$

$$= \int_{-\infty}^{\infty}\frac{d\omega}{2\pi}\frac{1-\cos\omega t}{\omega^2}\coth\frac{\beta\hbar\omega}{2}C_{\mu\nu}(\omega) + i\int_{-\infty}^{\infty}\frac{d\omega}{2\pi}\frac{\sin\omega t-\omega t}{\omega^2}C_{\mu\nu}(\omega). \tag{60}$$

Following Ref. 19, the exciton spectral density is given as

$$C_{\mu\nu}(\omega) \equiv \frac{1}{2}\int_{-\infty}^{\infty} dt\exp[i\omega t]\langle[q^{(c)}_{\mu\mu}(t), q^{(c)}_{\nu\nu}(0)]\rangle \tag{61}$$

$$= \sum_{m,n,k,l}\phi_\mu(m)\phi^*_\mu(n)\phi_\nu(k)\phi^*_\nu(l)C_{mn,kl}(\omega), \tag{62}$$

where the monomer spectral density is defined as

$$C_{mn,kl}(\omega) \equiv \frac{1}{2}\int_{-\infty}^{\infty} dt\exp[i\omega t]\tilde{C}_{mn,kl}(t). \tag{63}$$

Here, $\tilde{C}_{mn,kl}(t)=\langle[q^{(c)}_{mn}(t), q^{(c)}_{kl}(0)]\rangle$. The statistical average $\langle\ldots\rangle$ is integrated over $\exp[-\beta H_{\mathrm{ph}}(\{q_j\})]/Z$. As shown in Ref. 17, we find

$$\langle\hat{B}_\nu(\tau_4)\hat{B}^\dagger_\nu(\tau_3)\hat{B}_\mu(\tau_2)\hat{B}^\dagger_\mu(\tau_1)\rangle = e^{i(\tau_3-\tau_4)\epsilon_\nu+i(\tau_1-\tau_2)\epsilon_\mu}\exp[-g_{\nu\nu}(\tau_4-\tau_3) + g_{\nu\mu}(\tau_4-\tau_2) - g_{\nu\mu}(\tau_4-\tau_1) - g_{\nu\mu}(\tau_3-\tau_2) + g_{\nu\mu}(\tau_3-\tau_1) - g_{\mu\mu}(\tau_2-\tau_1)] \tag{64}$$

and

$$\langle\hat{B}_\nu(\tau_4)\hat{B}^\dagger_\nu(\tau_3)\hat{Y}_{\bar{\mu}}(\tau_3)\hat{Y}^\dagger_{\bar{\mu}}(\tau_2)\hat{B}_\mu(\tau_2)\hat{B}^\dagger_\mu(\tau_1)\rangle = e^{i(\tau_3-\tau_4)\epsilon_\nu+i(\tau_2-\tau_3)\epsilon_{\bar{\mu}}+i(\tau_1-\tau_2)\epsilon_\mu} \times\exp[-g_{\nu\nu}(\tau_4-\tau_3) + g_{\nu\bar{\mu}}(\tau_4-\tau_3) - g_{\nu\bar{\mu}}(\tau_4-\tau_2) + g_{\nu\mu}(\tau_4-\tau_2) - g_{\nu\mu}(\tau_4-\tau_1) + g_{\nu\bar{\mu}}(\tau_3-\tau_2) - g_{\nu\mu}(\tau_3-\tau_2) + g_{\nu\mu}(\tau_3-\tau_1) - g_{\bar{\mu}\bar{\mu}}(\tau_3-\tau_2) + g_{\bar{\mu}\mu}(\tau_3-\tau_2) - g_{\bar{\mu}\mu}(\tau_3-\tau_1) + g_{\bar{\mu}\mu}(\tau_2-\tau_1) - g_{\mu\mu}(\tau_2-\tau_1)]. \tag{65}$$

From these results, one can deduce that the window function

in Eq. (53) can be written in terms of the exciton line shape functions, that is,

$$W^L_{\mu\nu}(t_3) = \delta_{\mu a}\delta_{\nu b} d_a d_b e^{-i\epsilon_a t_3} \exp[-g_{aa}(t_3)] + \delta_{\mu a}\delta_{\nu b}\sum_{\bar{a}} d_{a\bar{a}} d_{b\bar{a}} e^{-i\epsilon_a t_3 + i\epsilon_{\bar{a}} t_3} \exp[-g_{\bar{a}\bar{a}}(-t_3) + g_{\bar{a}a}(-t_3) + g_{\bar{a}a}(t_3) - g_{aa}(t_3)]. \quad (66)$$

It is interesting to note that the doorway and window function components that are associated with the two-exciton coherent state, i.e., the last two terms in Eqs. (48) and (49), are not important, as well be shown in the following section.

VII. EXPLICIT EXPRESSIONS OF THE KERNEL FUNCTION

We derive here the explicit form of the kernel function in Eq. (42). It can be reexpressed as

$$K_{\lambda\alpha} = -\delta_{\nu\xi}\,\mathrm{Tr}[(\hat{B}^\dagger_\mu \hat{B}_\nu)^\dagger \mathsf{Q}_{\mu\nu}\hat{H}_1(\mathsf{P}\hat{H}_1\rho_{\chi\xi})] + \delta_{\mu\xi}\,\mathrm{Tr}[(\hat{B}^\dagger_\mu \hat{B}_\nu)^\dagger \mathsf{Q}_{\mu\nu}(\mathsf{P}\hat{H}_1\rho_{\chi\xi})\hat{H}_1] + \delta_{\nu\chi}\,\mathrm{Tr}[(\hat{B}^\dagger_\mu \hat{B}_\nu)^\dagger \mathsf{Q}_{\mu\nu}\hat{H}_1(\mathsf{P}\rho_{\chi\xi}\hat{H}_1)] - \delta_{\mu\chi}\,\mathrm{Tr}[(\hat{B}^\dagger_\mu \hat{B}_\nu)^\dagger \mathsf{Q}_{\mu\nu}(\mathsf{P}\rho_{\chi\xi}\hat{H}_1)\hat{H}_1], \quad (67)$$

where we set $\lambda=\mu\nu$ and $\alpha=\chi\xi$ on the right-hand side. The summation over α in Eq. (43) now corresponds to the summations over χ and ξ. Note that χ and ξ represent one-exciton states and that the kernel function [Eq. (42)] vanishes for $\lambda=\bar{\mu}0$ or $0\bar{\mu}$. The proof is given in Appendix C. Therefore, we can ignore all the contributions from the double exciton coherence transfer processes. That is to say, $D^L_{\bar{\mu}'}(t_1)$ in Eq. (51) and $W^L_{\bar{\mu}\bar{\nu}}(t_3)$ in Eq. (55) do not play any role. Substituting the perturbative Hamiltonian [Eq. (6)] into the kernel function, we obtain

$$K_{\lambda\alpha} = -\delta_{\nu\xi}\,\mathrm{Tr}[(\hat{B}^\dagger_\mu \hat{B}_\nu)^\dagger q^{(c)}_{\mu\nu}\hat{B}^\dagger_\mu \hat{B}_\nu q^{(c)}_{\nu\chi}\hat{B}^\dagger_\nu \hat{B}_\chi \rho_{\chi\xi}] + \delta_{\mu\xi}\,\mathrm{Tr}[(\hat{B}^\dagger_\mu \hat{B}_\nu)^\dagger q^{(c)}_{\mu\chi}\hat{B}^\dagger_\mu \hat{B}_\chi \rho_{\chi\xi} q^{(c)}_{\xi\nu}\hat{B}^\dagger_\xi \hat{B}_\nu] + \delta_{\nu\chi}\,\mathrm{Tr}[(\hat{B}^\dagger_\mu \hat{B}_\nu)^\dagger q^{(c)}_{\mu\chi}\hat{B}^\dagger_\mu \hat{B}_\chi \rho_{\chi\xi} q^{(c)}_{\xi\nu}\hat{B}^\dagger_\xi \hat{B}_\nu] - \delta_{\mu\chi}\,\mathrm{Tr}[(\hat{B}^\dagger_\mu \hat{B}_\nu)^\dagger \rho_{\chi\xi} q^{(c)}_{\chi\mu}\hat{B}^\dagger_\xi \hat{B}_\mu q^{(c)}_{\mu\nu}\hat{B}^\dagger_\mu \hat{B}_\nu] \quad (68)$$

$$= -\delta_{\nu\xi}\langle q^{(c)}_{\mu\nu} q^{(c)}_{\nu\chi}\rangle + \delta_{\nu\chi}\langle q^{(c)}_{\xi\nu} q^{(c)}_{\mu\chi}\rangle + \delta_{\mu\xi}\langle q^{(c)}_{\xi\nu} q^{(c)}_{\mu\chi}\rangle - \delta_{\mu\chi}\langle q^{(c)}_{\xi\mu} q^{(c)}_{\mu\nu}\rangle. \quad (69)$$

The above kernel function does not depend on time, so that the Green's function obeying Eq. (43) evolves with the constant rates $K_{\lambda\alpha}$. The constancy of the EECT rate kernel function originated from Eq. (36). This fact has not been reported before because former studies only considered EPT; note that the rate kernel for EPT are, in general, time dependent. This difference is due to the distinct characteristics of the Q-projection operator from those of the P-projection operator.

VIII. NONLINEAR RESPONSE FUNCTION AND FOUR-WAVE-MIXING SPECTROSCOPY

In impulsive three-pulse experiments, the incoming field is approximated as

$$E(\mathbf{r},\tilde{t}) = E_1\delta(\tilde{t}-(t_d-t-T-\tau))\{e^{i\mathbf{k}_1\cdot\mathbf{r}-i\omega_1\tilde{t}} + e^{-i\mathbf{k}_1\cdot\mathbf{r}+i\omega_1\tilde{t}}\} + E_2\delta(\tilde{t}-(t_d-t-T))\{e^{i\mathbf{k}_2\cdot\mathbf{r}-i\omega_2\tilde{t}} + e^{-i\mathbf{k}_2\cdot\mathbf{r}+i\omega_2\tilde{t}}\} + E_3\delta(\tilde{t}-(t_d-t))\{e^{i\mathbf{k}_3\cdot\mathbf{r}-i\omega_3\tilde{t}} + e^{-i\mathbf{k}_3\cdot\mathbf{r}+i\omega_3\tilde{t}}\}, \quad (70)$$

provided the rotating-wave approximation is invoked. Here, E_i denotes the ith pulse amplitude and t_d is the detection time. We will focus on a specific four-wave-mixing experiment where the signal is detected at time $t_d=t$ in the direction $\mathbf{k}_s=-\mathbf{k}_1+\mathbf{k}_2+\mathbf{k}_3$, which is called photon echo.[25] The corresponding third-order polarization[21]

$$P^{(3)}(\mathbf{r},t,T,\tau) = \int_0^\infty dt_3\int_0^\infty dt_2\int_0^\infty dt_1 R^{(3)}(t_3,t_2,t_1) \times E(\mathbf{r},t-t_3)E(\mathbf{r},t-t_3-t_2) \times E(\mathbf{r},t-t_3-t_2-t_1) \quad (71)$$

leads to

$$P^{(3)}(\mathbf{r},t,T,\tau) = P^{(3)}_{\mathbf{k}_s}(t,T,\tau)e^{i(-\mathbf{k}_1+\mathbf{k}_2+\mathbf{k}_3)\cdot\mathbf{r}}e^{i(\omega_1-\omega_2-\omega_3)t}, \quad (72)$$

where

$$P^{(3)}_{\mathbf{k}_s}(t,T,\tau) \equiv R^{(3)}(t,T,\tau)E_1E_2E_3e^{-i\omega_1(t+T+\tau)+i\omega_2(T+t)+i\omega_3 t}. \quad (73)$$

We can specify the Liouville paths which contribute to the above $R^{(3)}(t,T,\tau)$ (see Fig. 2). The two contributions associated with the Liouville paths (a) and (b) in Fig. 2 to $R^{(3)}(t,T,\tau)$ are

$$-i\sum_{\mu,\nu,\mu',\nu'} d_\mu d_\nu e^{i\varepsilon_\mu t}\exp[-g_{\mu\mu}(-t)] \times \tilde{G}_{\mu\nu\mu'\nu'}(T)d_{\mu'}d_{\nu'}e^{-i\varepsilon_{\mu'}\tau}\exp[-g_{\mu'\mu'}(\tau)] \quad (74)$$

and

$$i\sum_{\mu,\nu,\mu',\nu',\bar{\mu}} d_{\mu\bar{\mu}}d_{\nu\bar{\mu}}e^{-i\varepsilon_\mu t+i\varepsilon_{\bar{\mu}}t}\exp[-g_{\bar{\mu}\bar{\mu}}(-t) + g_{\bar{\mu}\mu}(-t) + g_{\bar{\mu}\mu}(t) - g_{\mu\mu}(t)]\tilde{G}_{\mu\nu\mu'\nu'}(T)d_{\mu'}d_{\nu'}e^{-i\varepsilon_{\mu'}\tau} \times\exp[-g_{\mu'\mu'}(\tau)], \quad (75)$$

respectively. $\tilde{G}_{\lambda\lambda'}(T)$ with $\lambda=\mu\nu$ and $\lambda'=\mu'\nu'$ can be calculated by the time-evolution equation [Eq. (43)] with the kernel function [Eq. (69)] and the initial conditions $\tilde{G}_{\lambda\lambda'}(0)=\delta_{\lambda,\lambda'}$.

IX. AN APPLICATION TO THE MOLECULAR AGGREGATE: B850 LH2 SYSTEM

We shall specifically consider the B850 LH2 system consisting of 18 B850 chlorophylls in a cyclic aggregate. We compared our results with those of Zhang *et al.*, where only EPT was taken into account.

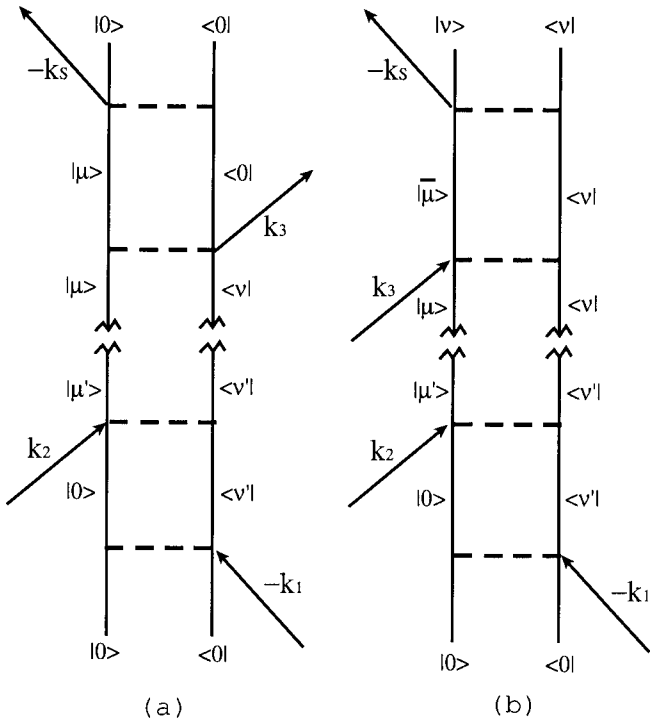

FIG. 2. Double-sided Feynman diagrams representing four-wave-mixing photon echo Liouville paths. The exciton-exciton coherence transfer (EECT) occurs during the time interval T between second and third pulses. The diagram (a) includes only single exciton states, while (b) contains the double exciton state.

It is well known that this cyclic aggregate has two kinds of nearest-neighbor intermolecular interactions; that is, the two coupling strengths between adjacent B850 chlorophylls in LH2 are −273 and −291 cm^{-1}, as determined in Ref. 26. For numerical calculations, we assume that the disorder of monomer excitation energy is specified by a Gaussian distribution,

$$f(\Omega_m) = \exp\left[-\frac{(\Omega_m - \tilde{\Omega}_m)^2}{\bar{\Omega}_m^2}\right], \tag{76}$$

with the characteristic eigenenergy of B850 chlorophylls $\tilde{\Omega}_m = 11\,710\ cm^{-1}$ and the full width at half maximum $\sigma = 2\sqrt{\log 2}\bar{\Omega}_m = 325\ cm^{-1}$. We further assume that the collective phonon variables acting on different monomers are statistically uncorrelated and have the same spectral density, that is,

$$C_{mn,kl}(\omega) = \delta_{mn}\delta_{kl}\delta_{mk}C(\omega). \tag{77}$$

In the present work, we use the spectral density of an overdamped Brownian oscillator,[11]

$$C(\omega) = 2\kappa\frac{\omega\tau_B}{\omega^2\tau_B^2 + 1}, \tag{78}$$

which generates the exponentially decayed correlated noise with the relaxation time $\tau_B = 130$ fs. The parameter $\kappa = 600\ cm^{-1}$ corresponds to the nuclear reorganization energy and is related to the overall exciton-phonon coupling strength. All the calculations in this section will be performed with $T_B = 300$ K. It is confirmed that the homogeneous and inhomogeneous parameters, $\kappa = 600\ cm^{-1}$ and $\sigma = 325\ cm^{-1}$, can quantitatively reproduce the experimental linear absorption linewidth.[14]

Substitution of Eq. (78) into Eq. (69) leads to

$$\langle q_{\xi\nu}^{(c)} q_{\mu\chi}^{(c)}\rangle = \sum_m \phi_\xi(m)\phi_\nu^*(m)\phi_\mu(m)\phi_\chi^*(m)\langle q_{mm}^{(c)} q_{mm}^{(c)}\rangle \tag{79}$$

$$= \sum_m \phi_\xi(m)\phi_\nu^*(m)\phi_\mu(m)\phi_\chi^*(m)\ddot{g}_{mm}(0), \tag{80}$$

with the monomer line shape function

$$g_{mn}(t) \equiv \int_0^t d\tau' \int_0^{\tau'} d\tau'' \langle q_{mm}^{(c)}(\tau'') q_{nn}^{(c)}(0)\rangle \tag{81}$$

$$= \int_{-\infty}^{\infty} \frac{d\omega}{2\pi}\frac{1-\cos\omega t}{\omega^2}\coth\frac{\beta\hbar\omega}{2} C_{mm,nn}(\omega) + i\int_{-\infty}^{\infty}\frac{d\omega}{2\pi}\frac{\sin\omega t - \omega t}{\omega^2} C_{mm,nn}(\omega). \tag{82}$$

Now, the Green's function describing EECT processes in Eqs. (74) and (75) can be obtained by numerically solving the time-evolution equation [Eq. (43)] with $K_{\lambda\alpha}$ values obtained from Eq. (80). It should be mentioned that, in contrast to EPT, the EECT Green's function is always real since the kernel function is real. We next provide numerically calculated spectroscopic signals including EECT. All the results have been averaged over 3000 realizations of the static disorder, which is sufficient for the short-time signals. All the spectroscopic signals are scaled in order that the maxima become unity.

A. Time-resolved echoes (TREs)

First of all, the two-dimensional (2D) time-resolved echo signals $I_1(t_1,t_2,t_3) = |R^{(3)}(t_3,t_2,t_1)|^2$ with respect to t_1 and t_3 are plotted in Fig. 3. Figures 3(a) and 3(b) are the time-resolved echo (TRE) signals with and without the EECT contribution, respectively. The latter signal corresponds to the results of Zhang *et al.*[17] Note that both TRE spectra are diagonally elongated since τ_B, κ, and T_B we used in the calculation correspond to slow modulation of heat-bath modes. However, the latter is more elongated than the former. This is because EECT additionally included in the former case generates the fast decaying coherent state evolutions. Apparently, the EECT process should not be ignored to quantitatively describe the TRE signal within ultrafast time scales.

B. Photon echo peak shift (PEPS)

The photon echo peak shift (PEPS) was shown to be useful in measuring correlation amplitude between the two electronic coherent states during t_1 and t_3.[25] The time-integrated photon echo signal is given as

$$I_2(t_1,t_2) = \int_0^\infty |R^{(3)}(t_3,t_2,t_1)|^2 dt_3. \tag{83}$$

The PEPS of LH2 was experimentally measured by Jimenez *et al.*,[14] and Zhang *et al.*[17] compared their numerically cal-

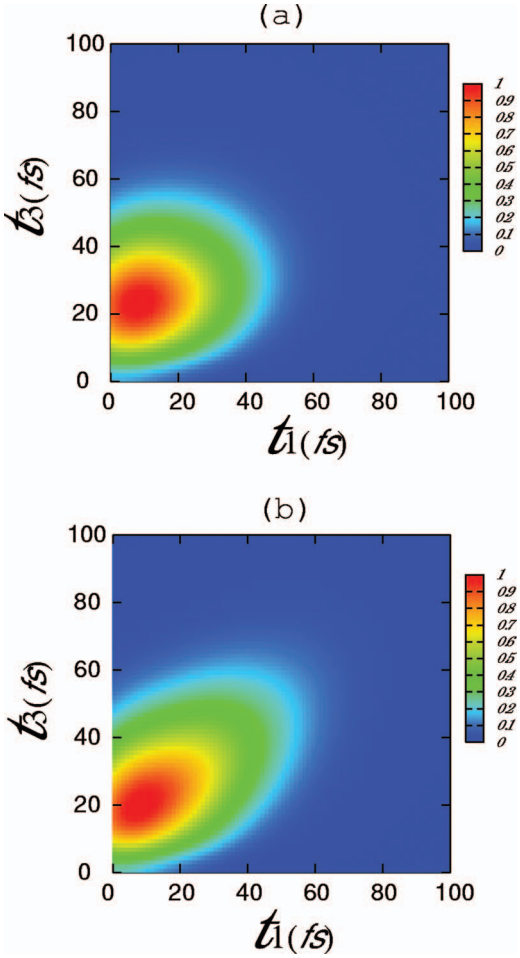

FIG. 3. (Color) The time-resolved echo (TRE) signals $|R^{(3)}(t_3,t_2,t_1)|^2$ vs t_1 and t_3 with $t_2=100$ fs with (a) and without (b) the EECT contribution. The fact that (b) is more elongated than (a) illustrates that EECT generates the fast decaying coherent state evolutions.

culated PEPS with the experiment. Here, including the EECT contribution to the photon echo signal, we calculated the PEPS of LH2 and directly compared it with experimental data as well as with our numerical result without EECT (see Fig. 4). As can be seen in Fig. 4, the calculated PEPS with

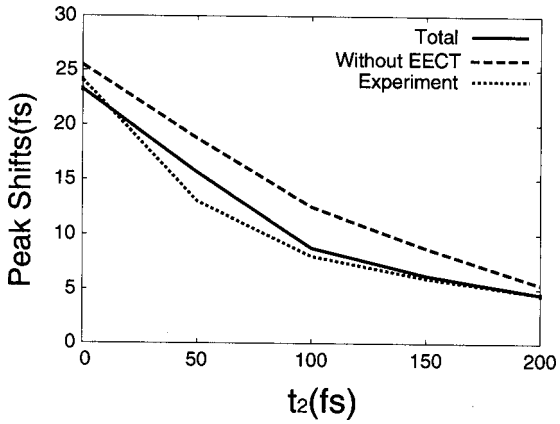

FIG. 4. Photon echo peak shifts (PEPSs) estimated from the time-integrated photon echo signals [Eq. (83)] with respect to t_2. The numerically calculated PEPSs with and without EECT are compared with the experimental results. The experimental data are measured in Ref. 14. The direct comparison shows that EECT is essential in accounting for the experimental data.

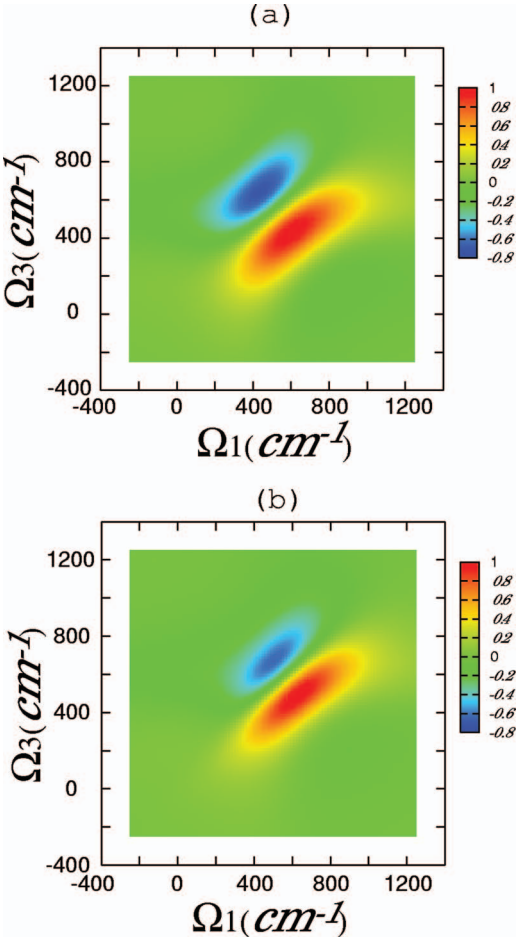

FIG. 5. (Color) (a) Real part of the 2D photon echo spectrum $I_3(\Omega_1,t_2,\Omega_3)$ in Eq. (84) at $t_2=100$ fs. The horizontal and vertical axes are $\Omega_1-\tilde{\Omega}_m$ cm^{-1} and $\Omega_3-\tilde{\Omega}_m$ cm^{-1}, respectively. Here, $\tilde{\Omega}_m=11\,710$ cm^{-1}, given in Eq. (76). (b) The same as in (a), but without EECT. The width along the antidiagonal axis of (a) is broader than that of (b). This means that the decoherence (memory loss) of multiple quantum coherent states is another source of homogeneous dephasing process. EECT can cause the rapid *diffusion* of frequencies.

EECT is in an excellent agreement with the experiment. It should be noted that the PEPS with EECT decays faster than that without EECT. This result can be understood by suggesting that the EECT during t_2 can induce decoherence (memory loss) of the multiple quantum coherent states created by the field-matter interactions.

C. Two-dimensional photon echo

We next calculate the two-dimensional photon echo spectrum by taking the double Fourier transformation of the time-resolved photon echo signals. Figures 5(a) and 5(b) depict the real parts of the 2D Fourier-transformed spectra with and without the EECT contribution, respectively. The latter signal corresponds to the results of Zhang *et al.*[17] Here, the definition of the 2D Fourier-transformed spectrum is

$$I_3(\Omega_1,t_2,\Omega_3)=\int_0^\infty\int_0^\infty \exp(i\Omega_1 t_1)\exp(-i\Omega_3 t_3)\times R^{(3)}(t_3,t_2,t_1)dt_1dt_3. \quad (84)$$

In both cases, the real part of the 2D Fourier-transformed

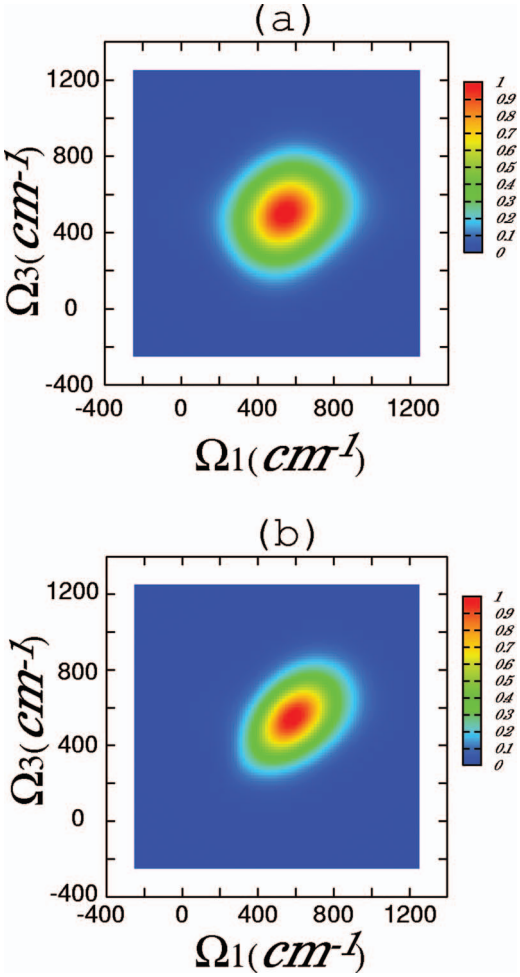

FIG. 6. (Color) (a) Absolute magnitude of the 2D photon echo spectrum $I_3(\Omega_1,t_2,\Omega_3)$ in Eq. (84) at $t_2=100$ fs. The horizontal and vertical axes are $\Omega_1-\tilde{\Omega}_m$ cm^{-1} and $\Omega_3-\tilde{\Omega}_m$ cm^{-1}, respectively. (b) The same as (a), but without EECT. The 2D correlation spectrum at an early time can be less diagonally elongated due to the decoherence of multiple quantum coherent states, i.e., hopping dephasing.

spectrum is diagonally elongated, indicating an inhomogeneous distribution (diagonal disorder) of the site energies. Secondly, the width along the antidiagonal axis of Fig. 5(a) is broader than that of Fig. 5(b). This means that the decoherence of multiple quantum coherent states is another source of a homogeneous dephasing process. In other words, EECT can cause the rapid *diffusion* of frequencies. We call this frequency diffusion *hopping dephasing* in order to distinguish it from the usual pure dephasing, which is due to static disorder and perturbative diagonal system-bath couplings. The difference between the two is discussed in Sec. X.

Examining the absolute magnitude of 2D Fourier-transformed spectra shown in Figs. 6(a) and 6(b), one can see clear evidence of the EECT contribution. In general, the diagonal disorder makes the 2D spectrum diagonally elongated.[27] However, as shown in the present studies, the 2D correlation spectrum at an early time can be less diagonally elongated due to the decoherence of multiple quantum coherent states, i.e., hopping dephasing.

X. DISCUSSION AND SUMMARY

In order to study the exciton-exciton coherence transfer (EECT) in strongly coupled molecular aggregates, we have developed a reduced time-evolution equation of EECT using the projection operator technique. Focusing on the Q space spanned by the set of coherent states, we have analyzed the nature of EECT by solving the integrodifferential equation for EECT. The relevant kernel was found to be determined by the cross correlation of the fluctuating coupling strengths induced by the system-bath interactions. We also obtained its explicit contribution to the nonlinear response function for a four-wave-mixing spectroscopy, e.g., photon echo. The doorway and window functions describing the preparation of population and coherent states and probing their time evolutions, respectively, were theoretically derived, and, particularly, the coherent state evolutions in the Q space were properly taken into consideration in this paper. As expected, it was shown that EECT plays a significant role in a strongly coupled molecular aggregate such as LH2.

Despite the fact that there already exist a number of theoretical works tackling the time-dependent optical responses of light-harvesting complexes, most of them have ignored contributions from EECT processes due to its ultrafast (approximately subpicosecond) nature.[28] As shown in this paper, EECT plays an important role in describing ultrafast transfer and decoherence phenomena in less than a few hundred femtoseconds. As an example, the short-time decaying pattern of the photon echo peak shift from LH2 was found to be critically dependent on the time scale of the EECT processes, as demonstrated in Fig. 4.

As emphasized in this paper, EECT involves coherent processes, contributes to the ultrafast spectroscopic signal, and appears as a rapid hopping dephasing inducing additional line broadening in the 2D photon echo spectrum. It should be noted that the hopping dephasing induced by EECT differs from the conventional pure dephasing. The latter makes the amplitude of a given coherent state monotonically decrease in time, whereas EECT can have a backward transfer process since EECT involves hopping among strongly correlated close coherent states. Because of rapid hopping motions among such close coherent states induced by the exciton-phonon interactions, only the hopping dephasing can destroy the quantum coherence rapidly. Theoretically, we showed that the EECT process cannot happen during τ and t periods because the corresponding kernel functions averaged over the phonon degrees of freedom vanish (Appendix B), whereas the pure dephasing is critical in describing τ and t dependencies of a nonlinear response function. Nevertheless, since we have fully included diagonal disorder effects as well as diagonal exciton-phonon couplings, our results contain effects of pure dephasing. Since the diagonal exciton-phonon coupling is treated nonperturbatively, the nuclear reorganization energy is properly incorporated in the present theory.

We have found that the transition rate kernel function of EECT is independent of time, which is not the case for EPT. Furthermore, since the kernel function of EECT has direct linear dependency on κ, which determines the overall mag-

nitude of spectral density and is linearly proportional to the fluorescence Stokes shift, the photon echo peak shifts including EECT were found to be more sensitive to the homogeneous dephasing parameter than those without EECT. This indicates that the parameter κ determining the homogeneous line-broadening process is an important factor for both EPT and EECT in a molecular aggregate and also in determining their relative weights. It is well known that conventional EPT rate constants are determined by the extent of overlap between probability densities of two different exciton states[7,19,29] as well as the spectral density at $\hbar\Omega_{jk}$, which is the energy gap between the jth and kth exciton states. As also seen in the detailed balance condition, there is a temperature dependent factor of $\exp(-\hbar\Omega_{jk}/k_BT_B)$, which indicates that the EPT rate is exponentially temperature dependent. In other words, the population transfer rate kernel depends on the time-dependent fluctuating bath-mode correlation function that is exponentially dependent on thermal energy, k_BT_B. Indeed, as we discussed in Sec. IV, highly fluctuating coherent states appear in the population transfer process due to its coupling to the bath degrees of freedom. This fact implies the more sensitive temperature dependency of the EPT kernel function. On the other hand, the EECT kernel function is less susceptible to T_B since the Boltzmann factor does not appear in the expression for the EECT rate function.

Finally, we would like to mention a few limitations of the present theory which arise from few approximations invoked in the present theoretical work. By introducing the thermal averaging of the doorway and window functions separately, we neglected the long-time correlation of the system–heat bath interaction modes during the propagation time T. Similarly, the rate kernel function was obtained by taking separate ensemble averages of Eq. (B17) to obtain Eq. (43) over the harmonic heat-bath modes. We assumed that the spectral densities of all chromophores are identical and uncorrelated to each other, but in the future it may be desirable to use nonuniform and correlated spectral densities. Additionally, an anharmonicity of heat-bath modes, nonlinear system-bath couplings, and instability of a coherent state might not be negligible. By far, the most challenging issue is to develop a nonperturbative way to include EECT contribution to the nonlinear response function in the future.[11,30]

ACKNOWLEDGMENTS

This research is partially supported by Grant-in-Aids for Scientific Research from Japan Society for the Promotion of Science, Grant Nos. 17740278 and A 15205005. One of the authors (M.C.) is grateful for financial support from the CRI program of KOSEF (MOST, Korea). Another author (K.H.-D.) also appreciates useful technical support from T. Hasegawa and fruitful discussion with A. Kimura.

APPENDIX A: EXPLICIT EXPRESSIONS OF $\hat{G}(t_2)$

We have the following identity:[22,23]

$$\hat{G}(t_2) = \exp[-i(\hat{L}_0+\hat{L}_1)t_2]$$
$$= e^{-i\hat{L}_0t_2} - i\int_0^{t_2} dt e^{-i\hat{L}_0(t_2-t)}\hat{L}_1 e^{-i\hat{L}_0t}$$
$$- \int_0^{t_2} dt'' \int_0^{t''} dt' e^{-i\hat{L}_0(t_2-t'')}\hat{L}_1 e^{-i\hat{L}_0(t''-t')}\hat{L}_1 e^{-i\hat{L}t'}. \quad \text{(A1)}$$

Using the useful formulas $\hat{L}_0\mathsf{P}=\mathsf{P}\hat{L}_0=0$, $\mathsf{P}\hat{L}_1\mathsf{P}=0$, and $\mathsf{PQ}=\mathsf{QP}=0$, we find

$$\hat{G}_{\mathsf{PQ}}(t_2) = -i\int_0^{t_2} dt\mathsf{P}e^{-i\hat{L}_0(t_2-t)}(\mathsf{P}+\mathsf{Q})\hat{L}_1(\mathsf{P}+\mathsf{Q})e^{-i\hat{L}_0t}\mathsf{Q} \quad \text{(A2)}$$

$$\simeq -i\int_0^{t_2} dt\mathsf{P}e^{-i\hat{L}_0(t_2-t)}\mathsf{P}\hat{L}_1\mathsf{Q}e^{-i\hat{L}t}\mathsf{Q} \sim O(\hat{L}_1) \quad \text{(A3)}$$

to the lowest order of $\hat{L}_1$. In the third equation, we added $\hat{L}_1$ in the last exponential function of the integrand, which is the same assumption made in Ref. 22. Similarly, we have

$$\hat{G}_{\mathsf{QP}}(t_2) = -i\int_0^{t_2} dt\mathsf{Q}e^{-i\hat{L}_0(t_2-t)}(\mathsf{P}+\mathsf{Q})\hat{L}_1(\mathsf{P}+\mathsf{Q})e^{-i\hat{L}_0t}\mathsf{P} \quad \text{(A4)}$$

$$\simeq -i\int_0^{t_2} dt\mathsf{Q}e^{-i\hat{L}(t_2-t)}\mathsf{Q}\hat{L}_1\mathsf{P}e^{-i\hat{L}_0t}\mathsf{P} \sim O(\hat{L}_1) \quad \text{(A5)}$$

and

$$\hat{G}_{\mathsf{PP}}(t_2) = \mathsf{P}e^{-i\hat{L}_0t_2}\mathsf{P} - \int_0^{t_2} dt'' \int_0^{t''} dt' \mathsf{P}e^{-i\hat{L}_0(t_2-t'')}$$
$$\times(\mathsf{P}+\mathsf{Q})\hat{L}_1(\mathsf{P}+\mathsf{Q})e^{-i\hat{L}_0(t''-t')}$$
$$\times(\mathsf{P}+\mathsf{Q})\hat{L}_1(\mathsf{P}+\mathsf{Q})e^{-i\hat{L}t'}\mathsf{P} \quad \text{(A6)}$$

$$\simeq \mathsf{P}e^{-i\hat{L}_0t_2}\mathsf{P} - \int_0^{t_2} dt'' \int_0^{t''} dt' \mathsf{P}e^{-i\hat{L}_0(t_2-t'')}$$
$$\times\mathsf{P}\hat{L}_1\mathsf{Q}e^{-i\hat{L}(t''-t')}\mathsf{Q}\hat{L}_1\mathsf{P}e^{-i\hat{L}_0t'}\mathsf{P} \sim O(\hat{L}_1^2). \quad \text{(A7)}$$

The above equations become exact when we consider an exciton system consisting of only two monomers. This is because $\mathsf{Q}L_1\mathsf{Q}=0$ holds for such a system.

APPENDIX B: SINGLE EXCITON COHERENCE TRANSFER IN MOLECULAR AGGREGATES

The SECT is discussed in this Appendix. It will be shown that the SECT contributions vanish as long as the heat bath is a collection of harmonic oscillators and the exciton-phonon coupling coefficients linearly depend on heat-bath coordinates.

1. Projection operator expression

With the unit operator $\mathsf{P}+\mathsf{Q}$ operating on $\hat{G}(t_1)$ and $\hat{G}(t_3)$, we have

$$\hat{G}(t_1) = (\mathsf{P}+\mathsf{Q})\hat{G}(t_1)(\mathsf{P}+\mathsf{Q}) \tag{B1}$$

$$= \hat{G}_{\mathsf{QQ}}(t_1) \tag{B2}$$

and

$$\hat{G}(t_3) = (\mathsf{P}+\mathsf{Q})\hat{G}(t_3)(\mathsf{P}+\mathsf{Q}) \tag{B3}$$

$$= \hat{G}_{\mathsf{QQ}}(t_3). \tag{B4}$$

It should be mentioned that during t_1 and t_3, the density matrix is in a coherent state off-diagonal density matrix such as $\hat{\rho}_{0\mu}$, $\hat{\rho}_{0\bar{\mu}}$, and $\hat{\rho}_{\mu\bar{\nu}}$. Thus, we only need to consider the elements of QQ in Eqs. (B2) and (B4). Substitution of $\hat{G}(t_1)$ and $\hat{G}(t_3)$ into Eq. (7) leads to

$$R^{(3)}(t_3,t_2,t_1) = i^3\,\mathrm{Tr}[\hat{d}\hat{G}_{\mathsf{QQ}}(t_3)\hat{d}^{\times}\hat{G}_{\mathsf{PP}}(t_2)\hat{d}^{\times}\hat{G}_{\mathsf{QQ}}(t_1)\hat{d}^{\times}\hat{\rho}_{00}] + i^3\,\mathrm{Tr}[\hat{d}\hat{G}_{\mathsf{QQ}}(t_3)\hat{d}^{\times}\hat{G}_{\mathsf{PQ}}(t_2)\hat{d}^{\times}\hat{G}_{\mathsf{QQ}}(t_1)\hat{d}^{\times}\hat{\rho}_{00}]$$
$$+ i^3\,\mathrm{Tr}[\hat{d}\hat{G}_{\mathsf{QQ}}(t_3)\hat{d}^{\times}\hat{G}_{\mathsf{QP}}(t_2)\hat{d}^{\times}\hat{G}_{\mathsf{QQ}}(t_1)\hat{d}^{\times}\hat{\rho}_{00}] + i^3\,\mathrm{Tr}[\hat{d}\hat{G}_{\mathsf{QQ}}(t_3)\hat{d}^{\times}\hat{G}_{\mathsf{QQ}}(t_2)\hat{d}^{\times}\hat{G}_{\mathsf{QQ}}(t_1)\hat{d}^{\times}\hat{\rho}_{00}]. \tag{B5}$$

To the second order with respect to $\hat{L}_1$, we have

$$R^{(3)}(t_3,t_2,t_1) = i^3\,\mathrm{Tr}[\hat{d}\hat{G}^0_{\mathsf{QQ}}(t_3)\hat{d}^{\times}\hat{G}^0_{\mathsf{PP}}(t_2)\hat{d}^{\times}\hat{G}_{\mathsf{QQ}}(t_1)\hat{d}^{\times}\hat{\rho}_{00}] + i^3\,\mathrm{Tr}[\hat{d}\hat{G}^0_{\mathsf{QQ}}(t_3)\hat{d}^{\times}\hat{G}^0_{\mathsf{QQ}}(t_2)\hat{d}^{\times}\hat{G}_{\mathsf{QQ}}(t_1)\hat{d}^{\times}\hat{\rho}_{00}]$$
$$+ i^3\,\mathrm{Tr}[\hat{d}\hat{G}_{\mathsf{QQ}}(t_3)\hat{d}^{\times}\hat{G}^0_{\mathsf{PP}}(t_2)\hat{d}^{\times}\hat{G}^0_{\mathsf{QQ}}(t_1)\hat{d}^{\times}\hat{\rho}_{00}] + i^3\,\mathrm{Tr}[\hat{d}\hat{G}_{\mathsf{QQ}}(t_3)\hat{d}^{\times}\hat{G}^0_{\mathsf{QQ}}(t_2)\hat{d}^{\times}\hat{G}^0_{\mathsf{QQ}}(t_1)\hat{d}^{\times}\hat{\rho}_{00}]. \tag{B6}$$

It is noted that the EECT processes during t_2 were discussed in the main text and that the zeroth-order terms in Eq. (B6), $i^3\,\mathrm{Tr}[\hat{d}\hat{G}^0_{\mathsf{QQ}}(t_3)\hat{d}^{\times}\hat{G}^0_{\mathsf{PP}}(t_2)\hat{d}^{\times}\hat{G}^0_{\mathsf{QQ}}(t_1)\hat{d}^{\times}\hat{\rho}_{00}]$ and $i^3\,\mathrm{Tr}[\hat{d}\hat{G}^0_{\mathsf{QQ}}(t_3)\hat{d}^{\times}\hat{G}^0_{\mathsf{QQ}}(t_2)\hat{d}^{\times}\hat{G}^0_{\mathsf{QQ}}(t_1)\hat{d}^{\times}\hat{\rho}_{00}]$ were already studied in detail in Ref. 17.

2. The doorway-window picture

Equation (B6) can now be rewritten as, in terms of the doorway and window functions,

$$R^{(3)}(t_3,t_2,t_1) = i^3\sum_{\lambda,\lambda'}\mathrm{Tr}[\hat{d}\hat{G}^0_{\mathsf{QQ}}(t_3)\hat{d}^{\times}\hat{G}^0_{\mathsf{PP}}(t_2)\hat{d}^{\times}\mathsf{Q}_{\lambda}\hat{G}(t_1)\mathsf{Q}_{\lambda'}\hat{d}^{\times}\hat{\rho}_{00}] + i^3\sum_{\lambda,\lambda'}\mathrm{Tr}[\hat{d}\hat{G}^0_{\mathsf{QQ}}(t_3)\hat{d}^{\times}\hat{G}^0_{\mathsf{QQ}}(t_2)\hat{d}^{\times}\mathsf{Q}_{\lambda}\hat{G}(t_1)\mathsf{Q}_{\lambda'}\hat{d}^{\times}\hat{\rho}_{00}]$$
$$+ i^3\sum_{\lambda,\lambda'}\mathrm{Tr}[\hat{d}\mathsf{Q}_{\lambda}\hat{G}(t_3)\mathsf{Q}_{\lambda'}\hat{d}^{\times}\hat{G}^0_{\mathsf{PP}}(t_2)\hat{d}^{\times}\hat{G}^0_{\mathsf{QQ}}(t_1)\hat{d}^{\times}\hat{\rho}_{00}] + i^3\sum_{\lambda,\lambda'}\mathrm{Tr}[\hat{d}\mathsf{Q}_{\lambda}\hat{G}(t_3)\mathsf{Q}_{\lambda'}\hat{d}^{\times}\hat{G}^0_{\mathsf{QQ}}(t_2)\hat{d}^{\times}\hat{G}^0_{\mathsf{QQ}}(t_1)\hat{d}^{\times}\hat{\rho}_{00}] \tag{B7}$$

$$= -i\sum_{\lambda,\lambda'}W^a_{\lambda}(t_3,t_2)\tilde{G}^S_{\lambda\lambda'}(t_1) - i\sum_{\lambda,\lambda'}W^b_{\lambda}(t_3,t_2)\tilde{G}^S_{\lambda\lambda'}(t_1) - i\sum_{\lambda,\lambda'}\tilde{G}^S_{\lambda\lambda'}(t_3)D^a_{\lambda'}(t_2,t_1) - i\sum_{\lambda,\lambda'}\tilde{G}^S_{\lambda\lambda'}(t_3)D^b_{\lambda'}(t_2,t_1), \tag{B8}$$

where λ and λ' denote the coherent states such as $\rho_{0\mu}$ and $\rho_{\mu\bar{\nu}}$. In Eq. (B8), we introduced the doorway functions

$$D^a_{\lambda'}(t_2,t_1) \equiv \mathrm{Tr}[\lambda'^{\dagger}\mathsf{Q}_{\lambda'}\hat{d}^{\times}\hat{G}^0_{\mathsf{PP}}(t_2)\hat{d}^{\times}\hat{G}^0_{\mathsf{QQ}}(t_1)\hat{d}^{\times}\hat{\rho}_{00}], \tag{B9}$$

$$D^b_{\lambda'}(t_2,t_1) \equiv \mathrm{Tr}[\lambda'^{\dagger}\mathsf{Q}_{\lambda'}\hat{d}^{\times}\hat{G}^0_{\mathsf{QQ}}(t_2)\hat{d}^{\times}\hat{G}^0_{\mathsf{QQ}}(t_1)\hat{d}^{\times}\hat{\rho}_{00}] \tag{B10}$$

and the window functions

$$W^a_{\lambda}(t_3,t_2) \equiv \mathrm{Tr}[\hat{d}\hat{G}^0_{\mathsf{QQ}}(t_3)\hat{d}^{\times}\hat{G}^0_{\mathsf{PP}}(t_2)\hat{d}^{\times}\hat{\rho}_{\lambda}], \tag{B11}$$

$$W^b_{\lambda}(t_3,t_2) \equiv \mathrm{Tr}[\hat{d}\hat{G}^0_{\mathsf{QQ}}(t_3)\hat{d}^{\times}\hat{G}^0_{\mathsf{QQ}}(t_2)\hat{d}^{\times}\hat{\rho}_{\lambda}]. \tag{B12}$$

$\lambda'^{\dagger}$ is necessary to generate the state $\rho_{\lambda'}$ in the following Green's function $\hat{G}^S_{\lambda\lambda'}(t_3)$. The Green's function, which reflects SECT, corresponds to the matrix element of $\hat{G}_{\mathsf{QQ}}(t)$,

$$\hat{G}^S_{\lambda\lambda'}(t) \equiv \mathsf{Q}_{\lambda}\hat{G}(t)\mathsf{Q}_{\lambda'}\hat{d}^{\times}\hat{\rho}_{00} = \mathsf{Q}_{\lambda}\hat{G}(t)\mathsf{Q}_{\lambda'}\hat{\rho}_{\lambda'}. \tag{B13}$$

This means the conditional probability for the coherent state to be in λ at time t when it starts at λ' at time $t=0$. We further introduce, in Eq. (B8),

$$\tilde{\hat{G}}^S_{\lambda\lambda'}(t) \equiv \lambda^{\dagger}\hat{G}^S_{\lambda\lambda'}(t) \tag{B14}$$

in order to cancel the state ρ_{λ} in the above $W^a_{\lambda}(t_3,t_2)$ and $W^a_{\lambda}(t_3,t_2)$ and to include the left P in the third and fourth terms of Eq. (B7)

3. The time-evolution equation of the Green's function

Since at time $t_1=0$ and $t_3=0$, the density matrix must have a coherent state, the time-evolution equation of the Q-projected density matrix [Eq. (34)] leads to

$$\frac{\partial \mathsf{Q}\rho(t)}{\partial t} = -i\mathsf{Q}\hat{L}\mathsf{Q}\rho(t) - \int_0^t d\tau \mathsf{Q}\hat{L}_1\mathsf{P}\hat{L}_1\mathsf{Q}\rho(\tau). \tag{B15}$$

Replacing the left Q with Q_λ and $\rho(t)$ with $e^{-i\hat{L}t}\mathsf{Q}_{\lambda'}\rho(0)$, Eq. (B15) gives

$$\frac{\partial \mathsf{Q}_\lambda e^{-i\hat{L}t}\mathsf{Q}_{\lambda'}\rho(0)}{\partial t} = -i\sum_\alpha \mathsf{Q}_\lambda\hat{L}\mathsf{Q}_\alpha e^{-i\hat{L}t}\mathsf{Q}_{\lambda'}\rho(0) - \sum_\alpha \int_0^t d\tau \mathsf{Q}_\lambda\hat{L}_1\mathsf{P}\hat{L}_1\mathsf{Q}_\alpha e^{-i\hat{L}\tau}\mathsf{Q}_{\lambda'}\rho(0) \tag{B16}$$

At last, we can derive the time-evolution equation of the SECT Green's function,

$$\frac{\partial \hat{G}^S_{\lambda\lambda'}(t)}{\partial t} = -i\sum_\alpha \mathsf{Q}_\lambda\hat{L}\hat{G}^S_{\alpha\lambda'}(t) - \sum_\alpha \int_0^t d\tau \mathsf{Q}_\lambda\hat{L}_1\mathsf{P}\hat{L}_1 G^S_{\alpha\lambda'}(\tau). \tag{B17}$$

In terms of $\tilde{\hat{G}}^S_{\lambda\lambda'}(t)$ in Eq. (B14), we obtain

$$\frac{\partial \tilde{G}^S_{\lambda\lambda'}(t)}{\partial t} = \sum_\alpha K^a_{\lambda\alpha}\tilde{G}^S_{\alpha\lambda'}(t) + \sum_\alpha \int_0^t d\tau K^b_{\lambda\alpha}\tilde{G}^S_{\alpha\lambda'}(\tau), \tag{B18}$$

with the kernel functions

$$K^a_{\lambda\alpha} \equiv -i\,\mathrm{Tr}[\lambda^\dagger\mathsf{Q}_\lambda\hat{L}\rho_\alpha] \tag{B19}$$

and

$$K^b_{\lambda\alpha} \equiv -\mathrm{Tr}[\lambda^\dagger\mathsf{Q}_\lambda\hat{L}_1\mathsf{P}\hat{L}_1\rho_\alpha]. \tag{B20}$$

4. Explicit calculations of the rate kernel functions

We derive explicit forms of the rate kernel functions [Eqs. (B19) and (B20)]. The rate kernel functions can be expressed as

$$\begin{aligned} K^a_{\lambda\alpha} = &-i\delta_{\mu\chi}\delta_{\nu\xi}\,\mathrm{Tr}[(\hat{B}^\dagger_\mu\hat{B}_\nu)^\dagger\mathsf{Q}_{\mu\nu}\hat{H}_0\rho_{\chi\xi}] \\ &+ i\delta_{\mu\chi}\delta_{\nu\xi}\,\mathrm{Tr}[(\hat{B}^\dagger_\mu\hat{B}_\nu)^\dagger\mathsf{Q}_{\mu\nu}\rho_{\chi\xi}\hat{H}_0] \\ &- i\delta_{\nu\xi}\,\mathrm{Tr}[(\hat{B}^\dagger_\mu\hat{B}_\nu)^\dagger\mathsf{Q}_{\mu\nu}\hat{H}_1\rho_{\chi\xi}] \\ &+ i\delta_{\mu\chi}\,\mathrm{Tr}[(\hat{B}^\dagger_\mu\hat{B}_\nu)^\dagger\mathsf{Q}_{\mu\nu}\rho_{\chi\xi}\hat{H}_1] \end{aligned} \tag{B21}$$

and

$$\begin{aligned} K^b_{\lambda\alpha} = &-\delta_{\nu\xi}\,\mathrm{Tr}[(\hat{B}^\dagger_\mu\hat{B}_\nu)^\dagger\mathsf{Q}_{\mu\nu}\hat{H}_1(\mathsf{P}\hat{H}_1\rho_{\chi\xi})] \\ &+ \delta_{\mu\xi}\,\mathrm{Tr}[(\hat{B}^\dagger_\mu\hat{B}_\nu)^\dagger\mathsf{Q}_{\mu\nu}(\mathsf{P}\hat{H}_1\rho_{\chi\xi})\hat{H}_1] \\ &+ \delta_{\nu\chi}\,\mathrm{Tr}[(\hat{B}^\dagger_\mu\hat{B}_\nu)^\dagger\mathsf{Q}_{\mu\nu}\hat{H}_1(\mathsf{P}\rho_{\chi\xi}\hat{H}_1)] \\ &- \delta_{\mu\chi}\,\mathrm{Tr}[(\hat{B}^\dagger_\mu\hat{B}_\nu)^\dagger\mathsf{Q}_{\mu\nu}(\mathsf{P}\rho_{\chi\xi}\hat{H}_1)\hat{H}_1], \end{aligned} \tag{B22}$$

where we set $\lambda=\mu\nu$ and $\alpha=\chi\xi$ on the right-hand side. The summation over α in Eq. (B18) now corresponds to the summations over χ and ξ. We note that during the intervals t_1 and t_3, $\mu\nu=0\nu$, $\mu 0$, $\bar{\mu}\nu$, and $\mu\bar{\nu}$. Substituting the nonperturbative and perturbative Hamiltonians [Eqs. (5) and (6)] into the kernel function [Eq. (B21)], we obtain

$$\begin{aligned} K^a_{\lambda\alpha} = &-i\delta_{\nu\xi}\sum_{\mu\nu}\mathrm{Tr}[(\hat{B}^\dagger_\mu\hat{B}_\nu)^\dagger q^{(c)}_{\mu\chi}\hat{B}^\dagger_\mu\hat{B}_\chi\rho_{\chi\xi}] \\ &+ i\delta_{\mu\chi}\sum_{\mu\nu}\mathrm{Tr}[(\hat{B}^\dagger_\mu\hat{B}_\nu)^\dagger\rho_{\chi\xi}q^{(c)}_{\xi\nu}\hat{B}^\dagger_\xi\hat{B}_\nu] \\ = &-i\delta_{\nu\xi}\langle q^{(c)}_{\mu\xi}\rangle + i\delta_{\mu\chi}\langle q^{(c)}_{\xi\nu}\rangle. \end{aligned} \tag{B23}$$

The first and second terms in Eq. (B21) vanish because they are canceled by each other. We emphasize that $K^a_{\lambda\alpha}$ results in zero as long as we adopt the harmonic bath and the coupling constant $q^{(c)}_{\mu\nu}$ is proportional to q_j due to Eq. (3). It can be said that if any contribution from SECT appeared, we could indicate that the heat-bath oscillators are not harmonic, or that the exciton-phonon coupling is not linearly proportional to the bath coordinates.

We next discuss $\mathsf{P}\hat{H}_1\rho_{\chi\nu}$ and $\mathsf{P}\rho_{\mu\chi}\hat{H}_1$ in $K^b_{\lambda\alpha}$ of Eq. (B22) and find that they vanish. This is because the coherent states during t_1 and t_3 include only $\rho_{0\mu}$, $\rho_{\mu\bar{\nu}}$, and their conjugates, and $\hat{H}_1$ in Eq. (6) cannot create the density matrix which does not vanish after the P operator.

Finally, we have the time-evolution equation of the Green's function as

$$\frac{\partial \tilde{G}^S_{\lambda\lambda'}(t)}{\partial t} = 0, \tag{B24}$$

which shows that $\tilde{G}^S_{\lambda\lambda'}(t)$ is zeroth order of $\hat{L}_1$. We therefore conclude that no exciton coherence transfer occurs during t_1 and t_3. In other words, $R^{(3)}(t_3,t_2,t_1)$ in Eq. (B6) results in $i^3\,\mathrm{Tr}[\hat{d}\hat{G}^0_{\mathsf{QQ}}(t_3)\hat{d}^\times\hat{G}^0_{\mathsf{PP}}(t_2)\hat{d}^\chi\hat{G}^0_{\mathsf{QQ}}(t_1)\hat{d}^\chi\hat{\rho}_{00}] + i^3\,\mathrm{Tr}[\hat{d}\hat{G}^0_{\mathsf{QQ}}(t_3)\hat{d}^\times\hat{G}^0_{\mathsf{QQ}}(t_2)\hat{d}^\chi\hat{G}^0_{\mathsf{QQ}}(t_1)\hat{d}^\chi\hat{\rho}_{00}]$, which have been already calculated in Ref. 17. We will not calculate and show any explicit forms of the doorway and window functions appearing in Eqs. (B9)–(B12). It is also unnecessary to give the application to a four-wave-mixing experiment.

APPENDIX C: THE KERNEL FUNCTION FOR THE DOUBLE EXCITON STATE

The kernel function [Eq. (42)] for the two-exciton state can be expressed as

$$\begin{aligned} K_{\lambda\alpha} = &-\delta_{0\xi}\,\mathrm{Tr}[\lambda^\dagger\mathsf{Q}_\lambda\hat{H}_1(\mathsf{P}\hat{H}_1\hat{\rho}_{\chi\xi})] \\ &+ \delta_{0\xi}\,\mathrm{Tr}[\lambda^\dagger\mathsf{Q}_\lambda(\mathsf{P}\hat{H}_1\hat{\rho}_{\chi\xi})\hat{H}_1] \\ &+ \delta_{0\chi}\,\mathrm{Tr}[\lambda^\dagger\mathsf{Q}_\lambda\hat{H}_1(\mathsf{P}\hat{\rho}_{\chi\xi}\hat{H}_1)] \\ &- \delta_{0\chi}\,\mathrm{Tr}[\lambda^\dagger\mathsf{Q}_\lambda(\mathsf{P}\hat{\rho}_{\chi\xi}\hat{H}_1)\hat{H}_1], \end{aligned} \tag{C1}$$

The summation over α in Eq. (43) now corresponds to the summations over χ and ξ. Note that the above χ in the upper line and ξ in the lower line mean two-exciton states. The above kernel function vanishes since P is operated after one coherence transfer by $\hat{H}_1$. We emphasize that $\hat{H}_1$ in Eq. (6) cannot make any population state even if it is operated at $\hat{\rho}_{\bar{\mu}0}$ and $\hat{\rho}_{0\bar{\mu}}$.

[1] T. Ritz, A. Damjanović, and K. Schulten, ChemPhysChem **3**, 243 (2002).
[2] G. R. Fleming and G. D. Scholes, Nature (London) **431**, 256 (2004).
[3] M. Yang, R. Agarwal, and G. R. Fleming, J. Photochem. Photobiol., A **142**, 107 (2001).
[4] G. D. Scholes, X. J. Jordanides, and G. R. Fleming, J. Phys. Chem. B **105**, 1640 (2001).
[5] H. Sumi, J. Phys. Chem. B **103**, 252 (1999).
[6] H. Sumi, J. Lumin. **87**, 71 (2000).
[7] M. Yang and G. R. Fleming, Chem. Phys. **282**, 163 (2002).
[8] M. Yang, A. Damjanović, H. M. Vaswani, and G. R. Fleming, Biophys. J. **85**, 140 (2003).
[9] V. May and O. Kühn, *Charge and Energy Transfer Dynamics in Molecular Systems* (Wiley-VCH, New York, 2000).
[10] A. Nitzan, *Chemical Dynamics in Condensed Phases* (Oxford University Press, New York, 2006).
[11] Y. Tanimura, J. Phys. Soc. Jpn. **75**, 082001 (2006).
[12] V. Chernyak and S. Mukamel, J. Chem. Phys. **105**, 4565 (1996).
[13] T. Meier, V. Chernyak, and S. Mukamel, J. Chem. Phys. **107**, 8759 (1997).
[14] R. Jimenez, F. van Mourik, J. Y. Yu, and G. R. Fleming, J. Phys. Chem. B **101**, 7350 (1997).
[15] J.-Y. Yu, Y. Nagasawa, R. van Grondelle, and G. R. Fleming, Chem. Phys. Lett. **280**, 404 (1997).
[16] T. Joo, Y. Jia, J.-Y. Yu, D. M. Jonas, and G. R. Fleming, J. Phys. Chem. **100**, 2399 (1996).
[17] W. M. Zhang, T. Meier, V. Chernyak, and S. Mukamel, J. Chem. Phys. **108**, 7763 (1998).
[18] T. Brixner, J. Stenger, H. M. Vaswani, M. Cho, R. E. Blankenship, and G. R. Fleming, Nature (London) **434**, 625 (2005).
[19] M. Cho, H. M. Vaswani, T. Brixner, J. Stenger, and G. R. Fleming, J. Phys. Chem. B **109**, 10542 (2005).
[20] Y. C. Cheng and R. J. Silbey, Phys. Rev. Lett. **96**, 028103 (2006).
[21] S. Mukamel, *Principles of Nonlinear Optical Spectroscopy* (Oxford University Press, New York, 1999).
[22] M. Toda and R. Kubo, *Toukeibutsurigaku*, 2nd ed. (Iwanami Syoten, Tokyo, 1978).
[23] R. Zwanzig, *Nonequilibrium Statistical Mechanics* (Oxford University Press, New York, 2001).
[24] V. Novoderezhkin, M. Wendling, and R. van Grondelle, J. Phys. Chem. B **107**, 11534 (2003).
[25] G. R. Fleming and M. Cho, Annu. Rev. Phys. Chem. **47**, 103 (1996).
[26] K. Sauer, R. J. Cogdell, S. M. Prince, A. Freer, N. W. Isaacs, and H. Scheer, Photochem. Photobiol. **64**, 564 (1996).
[27] K. Okumura, A. Tokmakoff, and Y. Tanimura, Chem. Phys. Lett. **314**, 488 (1999).
[28] S. H. Lin, C. H. Chang, K. K. Liang, R. Chang, Y. J. Shiu, J. M. Zhang, T.-S. Yang, M. Hayashi, and F. C. Hsu, Adv. Chem. Phys. **121**, 1 (2002).
[29] O. Kühn and V. Sundstrom, J. Chem. Phys. **107**, 4154 (1997).
[30] A. Ishizaki and Y. Tanimura, J. Phys. Soc. Jpn. **74**, 3131 (2005).